

amt-2019-506 - Answer to referee #1 (RC1)

We thank the referee for her/his comments which have enabled us to improve the manuscript.

The manuscript presents a novel and interesting technique to quantify the mineral dust concentration starting from calibrated multi-wavelengths absorption measurements. This manuscript deserves to be published in AMT. Below my comments.

General comments

1) The proposed technique assumes that BC particles are not contained in the coarse fraction. Can the authors explain how much is this assumption true? And how the presence of coarse BC affects the mineral dust concentration calculated from the proposed method? There is a comment about this point only at lines 510-514 in the manuscript.

Author's response: As highlighted by the reviewer, possible influence of BC on absorbing properties of coarse particles is an important point to be addressed in the paper. At first, BC concentrations in the coarse mode are expected to be very low, typically ranging 0.02-0.03 $\mu\text{g}/\text{m}^3$, which is 10 times lower compared to fine BC at remote marine locations of the Western/Eastern Mediterranean (Sciare et al., 2003; Mallet et al., 2016). Also, the lack of relationship between the $b_{\text{abs},370\text{nm}}$ (PM1) and $b_{\text{abs},370\text{nm}}$ (VI) (Figure 3) together with the strong relationship between $b_{\text{abs},370\text{nm}}$ (VI) and mineral dust (Figure 7) further supports the idea that dust - rather than BC - is controlling absorption in the coarse mode. Nevertheless, the proposed technique does not make any assumptions whether a fraction of BC is contained or not in the coarse fraction. In other words, the methodology does not exclude possible BC coagulating onto dust aerosols. The EF and MAC determined during the calibration campaign are site-specific (i.e. they are dependent of the dust source region). The MAC for Middle East, for example, would reflect the contamination of dust with intense black carbon emissions that is typical of the region. Variability of MAC results in the increased uncertainty of PM_{dust} as discussed in chapter 3.7. To decrease uncertainty in the determination of mineral dust concentration, different MAC values should be used for different dust source regions.

Changes to the manuscript: Section 3.7, Line 589: "Desert dust may mix with BC emissions and this is relevant especially at source regions, where concentrations are large enough for efficient coagulation between dust and BC to occur (Clarke et al., 2004; Rodriguez et al., 2011), with up to a third of carbonaceous particles internally mixed with mineral dust (Hand et al., 2010). The presence of BC on large dust particles will increase the MAC of the coarse fraction. The presence of BC on dust means, that for these source regions, larger MAC values will be used to convert the optical measurements into dust concentrations. BC present on dust particles contributes negligibly to the mass and the resulting increase in PM10 concentrations is due to dust mass only. The increased MAC of these coagulated particles is also the relevant climate parameter, as dust and BC need to be taken into account together when estimating the direct radiative efficiency of such particles. To reduce the uncertainty resulting from different MAC values, a mineral dust source location can be determined using back-trajectory analysis and an appropriate MAC should be used for each source location."

2) The authors should explain better the concept of using a virtual impactor to concentrate coarse particles in the AE33 tape. What it does actually mean? Why the simple formula $\text{Abs}_{\text{TSP}} - \text{Abs}_{\text{PM1}}$ cannot be used to estimate the absorption by dust in the UV? Is the use of the virtual impactor (VI) the way to increase the sensitivity of the technique for measuring the absorption by dust? And from this the need to estimate the enhancement factor (EF)? See another comment on this below.

Author's response: An explanation of the concept is added at the beginning of the section 3.

Changes to the manuscript: Section 3, Line 313: "The absorption of the fine aerosol fraction, dominated by BC, is usually much larger compared to the absorption in the coarse fraction, which contains mineral dust. In other words, $\text{Abs}(\text{TSP})$ is expected to be close to $\text{Abs}(\text{PM1})$. Subtracting these two signals close in absolute values (but with large uncertainties), would result in a close-to-zero number associated with a large measurement error. The proposed VI method takes advantage of the concentration of coarse particles using a virtual impactor to enhance the coarse fraction in the sample, and subtracts the absorption of the fine fraction (as the

VI sample contains the same amount of fine fraction as an ambient sample). To calculate the absorption of the coarse fraction, the concentration efficiency of the virtual impactor must be taken into account. ”

3) A mean value of 11 for the EF is used here. However, the estimated EF varies quite a lot (Figure 5b). Would it be feasible to measure on-line the EF? How much the uncertainty of EF affects the final result compared to the other sources of error? EF uncertainty affects the MAC uncertainty and consequently the mineral dust concentration estimated from the optical measurements (?).

Author’s response: We determined a mean value of EF being 11 with standard deviation of 2. The uncertainty of the calculated mineral dust concentration caused by using a constant value of EF is evaluated in Chapter 3.7: it is 18%. This value is comparable to the absorption measurement uncertainty of the AE33, but smaller than the 40% variability of the mineral dust chemical composition traced by the Fe/Ca ratio. The uncertainty in the determination of MAC depends on the standard error of EF, which is very small (0.023). On-line measurements of EF are possible, but would require additional instrumentation, for example an APS, and additional VI system not necessarily present at the sites of interest.

Changes to the manuscript: Section 3.7, Line 378: “This uncertainty can be reduced by using time-resolved measurements of EF or modifying the virtual impactor design to sharpen its response.”

4) The on-line compensation for filter loading works well (as expected) for PM1 but not for the AE33 connected to the VI. The correction is performed off-line and a mean *k* is determined and used to correct the data. This introduces an additional uncertainty. Please, comment on this.

Author’s response: Using constant parameter *k* value introduces additional uncertainty, but it is very difficult to assess it quantitatively. We attempt to quantify it as a part of the 18% uncertainty assumed for the AE33 measurements at 370 nm (Chapter 3.7).

5) Figure 6: Is the slight overestimation of the theoretical curve (red line) at 660 nm compared to the experimental one (black line) due to dust absorption in the near-IR? The fit is performed from 880 nm assuming an AAE of 1. Dust should also absorb in the IR, isn’t it?

Author’s response: Certain species which compose mineral dust show strong absorption in the UV-VIS part of the spectrum, the absorption in infrared is small (Utry et al., 2015). It is possible that the coarse fraction contains some black carbon contamination. If mineral dust would be externally mixed with fine black carbon, we would expect AAE of 1 in the red-IR spectral region. For mineral dust contaminated with black carbon the absorption depends a lot on mineral particle size (Scarnato et al., 2015); the spectral dependence of black carbon stuck to the surface of the mineral dust particles should be evaluated numerically to determine AAE. It is also possible that the scattering artefact of the filter measurement is responsible for the apparent absorption in the infrared. In filter photometers scattering adds to the measured attenuation so that about 1-2% of the scattering coefficient is seen as apparent absorption (Drinovec et al, 2015).

6) Please, expand the Conclusion section if possible.

Author’s response: Section 4 was expanded.

Changes to the manuscript: Section 4, Line 614: “We have demonstrated the potential of the method by showing its applicability at a regional background site in Agia Marina Xyliatou (Cyprus), frequently impacted by desert dust. We have shown how to determine the sample MAC and use it to quantify with high time resolution the contribution of desert dust to local PM_{10} concentrations.

Although black carbon contribution to the coarse mode is expected to be very small, mixture of dust and black carbon may potentially affect the MAC values determined by our methodology. On the other hand, it will not alter the capacity of our methodology to deliver high time resolution PM_{10} concentrations of dust. Instead, our measurement system will be calibrated with such aerosol mixture and a site-specific MAC value will be derived, that takes into account this mixing state. Our approach is particularly relevant when using dust optical properties in climate models which need to account for real-world MAC values to determine the heating of the atmosphere due to these aerosols.

The variability of our calibration methodology and therefore, the range of experimentally determined MAC values is currently investigated through long-term (multi-year) continuous observations at two regional background sites of the Mediterranean: Agia Marina Xyliatou (Cyprus) and Montseny (Spain). Such data will offer the unique opportunity to explore the factors controlling dust MAC values and in particular the influence of mineralogy of the different source regions (and especially their hematite and goethite content) and the potential impact of complex mixture of dust with black carbon.”

Abstract

Line 30: “.....highly time resolved on-line *detection* technique of *dust absorption*...”. And also *dust concentration*? Maybe it would be better using the word “*quantification*” rather than “*detection*”?

Author’s response: We agree.

Changes to the manuscript: Abstract, Line 28: “We build on previous work using filter photometers and present here for the first time a highly time resolved on-line technique for quantification of mineral dust concentration by coupling a high flow virtual impactor (VI) sampler that concentrates coarse particles with an aerosol absorption photometer (Aethalometer, model AE33).”

Introduction

Line 56: “Desert dust impacts industrial production to a degree that has been fictionalized (Herbert, 1965)...”. Interesting citation, but not very pertinent with the scientific data presented here. What do the authors mean for “industrial production”?

Author’s response: We have expanded the Introduction to highlight the economic effects exerted by dust. We have added the new references.

Changes to the manuscript: Chapter 1, Line 54. “Dust deposits on snow and ice increase the ion content in snow and snow water (Greilinger et al., 2018) and they exert a warming influence after deposition (Di Mauro et al., 2015). Desert dust impacts our health and economy. Saharan dust events have been shown to increase morbidity and have negative influence on health mainly through respiratory and cardiovascular effects (Middleton et al., 2008; Perez et al., 2012). The health effects of mineral dust are being considered in the context of regulation (WHO, 2018). Dust soiling of photovoltaics is a significant factor in energy production and decreases their output by up to several percent (Mani and Pillai, 2010). Desert dust is a hazard for air and road transport, can cause electric fields detrimental for communication, and impacts water quality and plants, when deposited, resulting in great economic cost (Middleton, 2017), leading to the fictionalization due to its importance (Herbert, 1965).”

Changes to the manuscript: References, line 777. Mani, M. and Pillai, R.: Impact of dust on solar photovoltaic (PV) performance: Research status, challenges and recommendations, *Renew. Sust. Energ. Rev.*, 14, 3124-3131, <https://doi.org/10.1016/j.rser.2010.07.065>, 2010.

Changes to the manuscript: References, line 784. Middleton, N. J.: Desert dust hazards: A global review, *Aeol. Res.*, 24, 56-63, <https://doi.org/10.1016/j.aeolia.2016.12.001>, 2017.

Line 68: “Daily time resolution of the described method has been validated.....”. Please, describe briefly the method.

Changes to the manuscript: Section 1, Line 71. “Daily time resolution of the described method has been validated with the chemical composition and positive matrix factorization (PMF): the PM10 concentration above the daily regional background monthly 40th percentile has been shown to correlate well with aluminum (as a tracer of mineral dust), and the mineral dust factor from a PMF analysis (Viana et al., 2010).

Line 92: “.....can be used to identify dust events....”. Another advantage of using high-time resolution optical measurements, as the Angstrom Exponent of SSA, is the possibility to detect dust resuspending in the local

atmosphere after the end of the episode (when there are no more air masses coming from African deserts). This has big implication for air quality. However, the Angstrom Exponent of SSA cannot be used to quantify the dust concentration whereas the proposed technique does. Maybe a comment on this could be added to the Introduction and Conclusion sections.

Author's response: We have added additional text to the Introduction.

Changes to the manuscript: Section 1, Line 96: "These measurements with high time resolution have shown that the optical properties can be used to identify dust events. Additionally, combining the back-trajectory analysis and the SSA wavelength dependence, one can possibly detect local resuspension of dust, which impacts local air quality. However, these methods cannot determine the contribution of desert dust to PM10 concentrations in a quantitative manner."

Lines 95-120: Here the authors present some previous techniques that can be used to quantify dust concentration in PM using dust aerosol absorption properties. It would be useful to explain what are the main advantages of using the technique proposed in this manuscript compared to the previous techniques. In which terms is the proposed technique innovative? For example, the proposed technique is also affected by problems such as the enhancement due to scattering from dust particles in the filter matrix. A sentence in the Abstract and/or Introduction could be useful.

Author's response: We extended a sentence in the Abstract and added additional explanation to the Introduction and uncertainty analysis (chapter 3.7).

Changes to the manuscript: Abstract, Line 28: "We build on previous work using filter photometers and present here for the first time a highly time resolved on-line technique for quantification of mineral dust concentration by coupling a high flow virtual impactor (VI) sampler that concentrates coarse particles with an aerosol absorption photometer (Aethalometer, model AE33)."

Changes to the manuscript: Section1, Line 129: "Previous work has used two-component models to infer dust concentrations sampling ambient air on a filter in filter absorption photometers. However, the determination of the optical absorption of pure mineral dust - when mixed with black carbon - is more difficult..."

Changes to the manuscript: Section 3.7, Line 568: "The influence of the scattering material in the filter matrix, already included in the measurement uncertainty, could be reduced by explicitly taking into account the contribution of the scattering coefficient to the apparent absorption coefficient. However, this would require the knowledge of the particle size distribution, as the cross-sensitivity to scattering of the filter-based measurement depends on the particle size (Drinovec et al., 2015)."

Section 2.2.2

Line 208: "... the obtained data was compensated using fixed k values as described in ...". Please, define " k " here too.

Changes to the manuscript: Section 2.2.2, Line 213: "Given that the on-line filter loading compensation was not working efficiently for the AE33 coupled with the virtual impactor (see section 3.3, below), the obtained data was compensated using fixed filter loading compensation parameter k values as described in the Supplement S2."

Lines 211-223 (equations 1 and 2): Please, provide more details about the constants presented in this part of the text. For example, how was the new BC MAC at 880 nm calculated? From $3.5/2.14 = 7.77/4.74$? What is the constant 1.57? Which type of filter tapes were used during the experiment?

Author's response: The AE33 measurement during the campaign were conducted using a filter described in Drinovec et al. (2015), as noted in the manuscript. The multiple-scattering parameter C in Drinovec et al. (2015) determined the AE33 filter C values relative to the value of the quartz filter, used in older AE31 instruments. This AE31 value was assumed to be 2.14 (Weingartner et al., 2003), but it was later recommended to use an AE31 value of 3.5 (WMO, 2016). We therefore renormalized the AE33 filter C value:

$$C_{\text{new}} = C_{\text{old}} * 3.5/2.14 = 2.57$$

$$\sigma_{\text{air,new}} = \sigma_{\text{air,old}} * C_{\text{old}}/C_{\text{new}} = 7.77 \text{ m}^2\text{g}^{-1} * 1.57/2.57 = 4.74 \text{ m}^2\text{g}^{-1}.$$

Changes to the manuscript: Section 2.2.2, Line 223: »The calculation of the absorption coefficient was updated from the Drinovec et al. (2015) following the WMO guideline (WMO, 2016): we updated the value of the filter multiple-scattering parameter C . The multiple-scattering parameter C in Drinovec et al. (2015) determined the AE33 filter C values relative to the value of the quartz filter, used in older AE31 instruments. This AE31 value was assumed to be 2.14 (Weingartner et al., 2003), but it was later recommended to use an AE31 value of 3.5 (WMO, 2016). The parameter $C = 1.57$ used for the AE33 filter (Drinovec et al., 2015) was renormalized using the same factor resulting in a new value $C = 2.57$. The mass absorption cross-section σ_{air} for black carbon was adjusted in the inverse manner to obtain the same BC . The new mass absorption cross section for black carbon σ_{air} at 880 nm is now $4.74 \text{ m}^2 \text{ g}^{-1}$ instead of $7.77 \text{ m}^2 \text{ g}^{-1}$:«

Line 226: The uncertainty of BC was estimated from the plots in Figure S7 as the standard deviation of the ratio $BC_{\text{tsp}}/BC_{\text{pm1}}$. From equation 2, this ratio is equal to $b\text{ATN}_{\text{tsp}}/b\text{ATN}_{\text{pm1}}$ for each wavelength. Consequently, this ratio should change depending on the relative proportion of dust and BC in the sampled air (especially in the UV). The higher the mineral dust concentration, the higher should be the ratio (at least in the UV). Isn't it? However, no correlation is observed in Figure S7a. Could the authors explain better this point?

Author's response: $BC_{1\text{TSP}}$ signal should be higher than $BC_{1\text{PM1}}$ due to the absorption of mineral dust present in the coarse fraction. This is reflected in the slight positive slope of the $BC_{1\text{TSP}}/BC_{1\text{PM1}}$ seen in Figure S7a. Because of the Aethalometer measurement uncertainty the fitting parameter error is very large: Slope = $0.0054 \pm 0.0087 \mu\text{g}^{-1} \text{ m}^3$. We qualitatively explain this as a very small contribution of dust to absorption in TSP relative to BC, measured with a relatively large uncertainty. This is also the reason why virtual impactor inlet is necessary to concentrate the dust in order to measure its absorption. The reviewer notes this just below.

If I well understand, the lack of correlation in Figure S7a is because the absorption is dominated by BC in TSP too (not only in PM1) due to the much higher MAC of BC compared to dust particles. From this, the need of using a VI to concentrate the dust particles (whereas the BC particles are collected with a CE of unity in the VI) thus allowing measuring the absorption properties of dust. This point is commented at lines 480-485. Maybe it would be better commenting this before, e.g. in the section 2.2.1 or section 3.1.

Author's response: The need to concentrate coarse particles is highlighted in Section 1. Line 129. An additional explanation was added at the beginning of section 3.

Changes to the manuscript: Section 3, Line 313: "The absorption of the fine aerosol fraction, dominated by BC, is usually much larger compared to the absorption in the coarse fraction, which contains mineral dust. In other words, $b_{\text{abs,TSP}}$ is expected to be close to $b_{\text{abs,PM1}}$. Subtracting these two signals close in absolute values (but with large uncertainties), would result in a close-to-zero number associated with a large measurement error. The proposed VI method takes advantage of the concentration of coarse particles using a virtual impactor to enhance the coarse fraction in the sample, and subtracts the absorption of the fine fraction (as the VI sample contains the same amount of fine fraction as an ambient sample). To calculate the absorption of the coarse fraction, the concentration efficiency of the virtual impactor must be taken into account."

However, based on the numbers provided in the manuscript, the dust absorption in TSP during the campaign is not negligible compared to the BC absorption: Thus, at 370 nm:

$$\langle \text{mineral dust} \rangle * \text{MAC}_{\text{dust}} = \text{Abs}_{\text{dust}} (8.1 * 0.24 = \mathbf{1.94})$$

$$\langle \text{BC} \rangle * \text{MAC}_{\text{BC}} = \text{Abs}_{\text{BC}} (0.39 * 11.2 = \mathbf{4.4}).$$

However, in Figure S7a a mineral dust concentration value of 15 mg/m^3 will lead to a dust absorption at 370 nm of 3.6 Mm^{-1} . Please, comment about this point.

Author's response: For simplicity we will discuss the topic using absorption coefficients in Table 2 which provides campaign averages for $b_{\text{abs},370\text{nm}}$ of 6.1 Mm⁻¹ for TSP compared to 5.6 Mm⁻¹ for PM1 which show 9% difference. This difference is much smaller than the uncertainty of 36%. For average PM1 absorption of 5.6 Mm⁻¹ the difference should become statistically significant at mineral dust concentrations above 8.4 µg/m³.

Changes to the manuscript: Section 3.3, Line 465: "The average difference between absorption for TSP and PM1 inlets is lower than expected from the (VI-PM1)/2 absorption value. This is a consequence of high measurement uncertainty of up to 18% during the campaign (as estimated comparing Aethalometers with different inlets, Supplement S3). Mineral dust absorption calculated from the difference between $b_{\text{abs},370\text{nm}}$ for TSP and PM1 of 0.6 Mm⁻¹ has an uncertainty 2.1 Mm⁻¹."

Line 336: "As shown in Figure 3 the absorption in TSP is closely related to the one of PM1".
Please, see my previous comment.

Author's response: The analysis in Supplement S3 shows that there is no significant difference between the absorptions measured by two Aethalometers with TSP and PM1 inlets.

Changes to the manuscript: Section 3.1, Line 356: "The differences are inside the measurement uncertainty of the Aethalometers (Supplement S3)."

Section 3.4

Figure 8b: The scatterplot was done using the mineral dust content in PM2.5-10. How is the scatterplot if PM10 is used instead of PM2.5-10? I'm asking in case only PM10 is analysed.

Author's response: For calculation of MAC we have used mineral dust contained in PM_{10-2.5} fraction. The resulting mineral dust concentration (equation 7) is the mineral dust concentration in the coarse fraction. To calculate mineral dust in PM₁₀, a correction factor (1.06) should be used as mentioned in the first paragraph of section 3.7. If mineral dust in PM₁₀ is used for the calibration then the resulting mineral dust concentration (equation 7) reports the mineral dust concentration in PM₁₀.

Line 471: The MAC from the fit is provided with a very low uncertainty (0.01). isn't too low? It should be higher given that there are important sources of error (BC, EF, k , ...). Maybe the fit should be performed with X-Y error bars.

Author's response: The MAC is reported with the fitting parameter standard error. The uncertainty of MAC is discussed in detail in chapter 3.7. Because of the variability of Ca and Fe content in mineral dust the uncertainty of MAC is about 40%.

Last (but not least) comment: Would it be possible to test this technique by simulating the mineral dust concentration (and comparing with the filters) using AE33 data collected during other dust events than those presented here? The data presented here are from April-May 2016. Do the authors have other (e.g. more recent) data (AE33 PM1 and VI) available to test the technique using the MAC and EF estimated in this manuscript?

Author's response: The method is currently being tested in Cyprus (Agia Marina station) and Northern Spain (Montseny station). These datasets will allow for determination of MAC and EF for different source locations. Using source-area specific parameters will lower the uncertainty in the determination of mineral dust concentrations. The results will be published in several separate manuscripts in preparation. The Conclusions section was updated.

Changes to the manuscript: Section 4, Line 627: "The variability of our calibration methodology and therefore, the range of experimentally determined MAC values is currently investigated through long-term (multi-year) continuous observations at two regional background sites of the Mediterranean: Agia Marina Xyliatou (Cyprus) and Montseny (Spain). Such data will offer the unique opportunity to explore the factors controlling dust MAC values and in particular the influence of mineralogy of the different source regions (and especially their hematite and goethite content) and the potential impact of complex mixture of dust with black carbon."

References

Mani, M. and Pillai, R.: Impact of dust on solar photovoltaic (PV) performance: Research status, challenges and recommendations, *Renew. Sust. Energ. Rev.*, 14, 3124-3131, <https://doi.org/10.1016/j.rser.2010.07.065>, 2010.

Middleton, N. J.: Desert dust hazards: A global review, *Aeol. Res.*, 24, 56-63, <https://doi.org/10.1016/j.aeolia.2016.12.001>, 2017.

Weingartner, E., Saathoff, H., Schnaiter, M., Streit, N., Bitnar, B., and Baltensperger, U.: Absorption of light by soot particles: determination of the absorption coefficient by means of aethalometers, *J. Aerosol Sci.*, 34, 1445–1463, doi:10.1016/S0021-8502(03)00359-8, 2003.

WMO, Report No. 227: WMO/GAW Aerosol Measurement Procedures, Guidelines and Recommendations, 2nd Edition, 2016, Geneva, WMO.

amt-2019-506 - Answer to referee #2 (RC3)

We thank the referee for her/his comments which have enabled us to improve the manuscript.

This work presents a novel on-line detection technique of dust absorption (named VI-PM1) by comparing a coupled high flow virtual impactor sampler with an Aethalometer (model AE33) with the absorption of the submicron aerosol fraction measured with the same absorption photometer. This method was applied for detecting desert dust and was tested in the field for a period of two months at a regional background site in the Eastern Mediterranean. Such new techniques are most valuable to the field and VI-PM1 is expected to provide valuable information about dust particles and their properties. The authors however need to emphasize more the limitations of the method especially under conditions that the mineral dust is contaminated with black carbon.

Author's response: The method uses a single MAC value to calculate mineral dust concentration from the absorption data. MAC for different source locations is affected both by the variation of mineral composition (see chapter 3.7) and also by the possible contamination by black carbon. We treat the mineral dust contaminated by BC as the mineral dust that is measured at the receptor site, including the possible contamination. The uncertainty due to variation of the MAC can be lowered by using source location specific MAC value.

Changes to the manuscript: Section 3.7, Line 589: "Desert dust may mix with BC emissions and this is relevant especially at source regions, where concentrations are large enough for efficient coagulation between dust and BC to occur (Clarke et al., 2004; Rodriguez et al., 2011), with up to a third of carbonaceous particles internally mixed with mineral dust (Hand et al., 2010). The presence of BC on large dust particles will increase the MAC of the coarse fraction. The presence of BC on dust means, that for these source regions, larger MAC values will be used to convert the optical measurements into dust concentrations. BC present on dust particles contributes negligibly to the mass and the resulting increase in PM10 concentrations is due to dust mass only. The increased MAC of these coagulated particles is also the relevant climate parameter, as dust and BC need to be taken into account together when estimating the direct radiative efficiency of such particles. To reduce the uncertainty resulting from different MAC values, a mineral dust source location can be determined using back-trajectory analysis and an appropriate MAC should be used for each source location."

Specific Comments

L 195: The effect of water uptake in the sampling line, as could occur in Cyprus in spring time due to high ambient temperatures and RH, would require a drying step prior to the aethalometers which is however not described here. On the other hand, the APS and the nephelometer were connected to a nafion providing measurements in dry conditions. How were data handled since different conditions were applied? What limitations may be introduced due to water uptake by the particles?

Author's response: Certain aerosol species are hygroscopic which cause the increase in particle size in increased RH. The most hygroscopic are salts (sea salt, nitrates and sulphates) and oxygenated organic compounds. Mineral dust and black carbon alone are not hygroscopic and thus (if not coated) not susceptible to changes of optical properties due to humidity changes. Aethalometer samples have not been dried, as stated in the manuscript. The station temperature was kept at 25+/-2 deg. C. During the campaign, the average ambient temperature was 20 deg. C with 35% relative humidity. Due to small differences between ambient and station temperatures, we did not apply any correction to the data.

L 341: In Fig. 3 there are some periods when PM1 measurements seem to be higher than TSP (e.g. 19 April). Can this be attributed to the unit to unit variability?

Author's response: Yes, the difference is attributed to the unit-to unit variability, which was quantified in the Supplement S3. It shows that measurement uncertainty at 370 nm is about 18%.

Changes to the manuscript: Section 3.1, Line 356: »The differences are inside the measurement uncertainty of the Aethalometers (Supplement S3). »

L. 350: Since the laboratory tests for the enhancement factor were originally performed with flows 75 and 1.5 lpm and 95 and 5 lpm, why did the flows were finally chosen to be 100 and 2 lpm?

Author's response: We wanted to obtain higher concentration efficiencies which depend on the ratio of the flows F_{in}/F_{out} . With the minimum sample flow through the AE33 of 2 lpm we chose F_{in} of 100 lpm. We used the calibration curve obtained at 75 lpm to 1.5 lpm which has the same theoretical concentration efficiency of 50.

Changes to the manuscript: Section 3.2, Line 372: "Using the minimum sample flow of AE33 of 2 lpm and maximum flow of the virtual impactor pump we obtained the maximum F_{in}/F_{out} ratio of 50.«

L. 357: It would be better the axis to be in μm rather than nm.

Author's response: The axis units on Figure 4 was changed to μm .

L 410: To my opinion babs, mineral dust is not appropriate to describe the right term of this equation. This would require that there is no BC in the coarse mode, it would fail to describe the possibility of internally mixed BC and dust particles. Once internally mixed, the particles would have different optical properties than those of pure dust (e.g. Scarnato et al., 2015). In the Eastern Mediterranean such a mixture is possible. I recommend to change the left term to bcoarse or similar. This applies to Equation 7 and the subscript of MAC as well. Overall, a short discussion should be dedicated to this issue, expanding the sentence in Line 510 and on.

Author's response: The absorption coefficient in Equation 6 represents all absorbing species in the coarse aerosol fraction, thus the caption can be changed from $b_{\text{abs, mineral dust}}$ to $b_{\text{abs, PM10-1}}$. The situation is different for $\text{MAC}_{\text{mineral dust, 370 nm}}$, which is calculated using reference mineral dust concentration and not coarse mass concentration. In the same way Equation 7 represents calculated mineral dust concentration and not coarse fraction mass concentration.

Changes to the manuscript: Equation 6 is changed to $b_{\text{abs, PM10-1}} = \frac{b_{\text{abs, VI}} - b_{\text{abs, PM1}}}{EF}$.

Author's response: As explained above, MAC is a property of the mineral dust sampled during the calibration campaign. The value is representative for the source region during the campaign. As observed during our measurement campaign, the dust was probably contaminated by black carbon. The uncertainty of the method can be further reduced by applying MAC values specific for each source region. The subject is being studied and will be reported in a separate article.

Changes to the manuscript: Section 3.4, Line 537: "Simulations show that black carbon stuck to the mineral dust particles can severely change its optical properties, but the effect depends on the particle size (Scarnato et al., 2015). Because of the differences in dust mineral composition and contamination with BC, we expect MAC to be source region specific."

Changes to the manuscript: Section 3.7, Line 589: "Desert dust may mix with BC emissions and this is relevant especially at source regions, where concentrations are large enough for efficient coagulation between dust and BC to occur (Clarke et al., 2004; Rodriguez et al., 2011), with up to a third of carbonaceous particles internally mixed with mineral dust (Hand et al., 2010). The presence of BC on large dust particles will increase the MAC of the coarse fraction. The presence of BC on dust means, that for these source regions, larger MAC values will be used to convert the optical measurements into dust concentrations. BC present on dust particles contributes negligibly to the mass and the resulting increase in PM10 concentrations is due to dust mass only. The increased MAC of these coagulated particles is also the relevant climate parameter, as dust and BC need to be taken into account together when estimating the direct radiative efficiency of such particles. To reduce the uncertainty resulting from different MAC values, a mineral dust source location can be determined using back-trajectory analysis and an appropriate MAC should be used for each source location."

Changes to the manuscript: References, Line 832: "Rodríguez, S., Alastuey, A., Alonso-Pérez, S., Querol, X., Cuevas, E., Abreu-Afonso, J., Viana, M., Pérez, N., Pandolfi, M., and de la Rosa, J.: Transport of desert dust mixed with North African industrial pollutants in the subtropical Saharan Air Layer, *Atmos. Chem. Phys.*, 11, 6663–6685, <https://doi.org/10.5194/acp-11-6663-2011>, 2011.

Changes to the manuscript: References, Line 836: “Scarnato, B. V., China, S., Nielsen, K., and Mazzoleni, C.: Perturbations of the optical properties of mineral dust particles by mixing with black carbon: a numerical simulation study, *Atmos. Chem. Phys.*, 15, 6913–6928, <https://doi.org/10.5194/acp-15-6913-2015>, 2015.”

References

Scarnato, B. V., China, S., Nielsen, K., and Mazzoleni, C.: Perturbations of the optical properties of mineral dust particles by mixing with black carbon: a numerical simulation study, *Atmos. Chem. Phys.*, 15, 6913–6928, <https://doi.org/10.5194/acp-15-6913-2015>, 2015.

References

Rodríguez, S., Alastuey, A., Alonso-Pérez, S., Querol, X., Cuevas, E., Abreu-Afonso, J., Viana, M., Pérez, N., Pandolfi, M., and de la Rosa, J.: Transport of desert dust mixed with North African industrial pollutants in the subtropical Saharan Air Layer, *Atmos. Chem. Phys.*, 11, 6663–6685, <https://doi.org/10.5194/acp-11-6663-2011>, 2011.

amt-2019-506 - Answer to referee #3 (RC2)

We thank the referee for her/his comments which have enabled us to improve the manuscript.

The paper presents a new technique relying on combining a virtual impactor with an eathalometer, and supports it with a substantial body of laboratory and field data, including both instrument characterization and intercomparisons. The technique under development has the potential to bring significant improvement to dust monitoring and characterization, especially in the context of mixed aerosol types. The text is well written and informative on the whole, but some stylistic detail should be improved, for example inconsistent use of different grammatical tenses (present, present perfect and past), making it difficult to differentiate between the authors' and previous work.

Some detail is not clear, potentially even leading to misunderstanding. For example, the introductory section is somewhat intidy, lacking a logical progression, and ought to be improved.

Author's response: We have taken all reviewer's comments in account and added to the Introduction to make it clearer.

The statement in lines 204-209 is unclear: is the nonlinearity due to filter saturation? And what are the "k values" - do they compensate for the nonlinearity? Are they constant over time, wavelength etc?

Author's response: The non-linearity caused by the filter loading effect is explained in Drinovec et al. (2015) article. The topic is quite extensive, for that reason it is kept out of this article.

Changes to the manuscript: Section 2.2.2, Line 213: "Given that the on-line filter loading compensation was not working efficiently for the AE33 coupled with the virtual impactor (see section 3.3, below), the obtained data was compensated using fixed filter loading compensation parameter k values as described in the Supplement S2."

In the Supplement, tests of the virtual impactor (VI) are carried out with PSL, which has specific gravity close to that of water, less that half of that of typical mineral dust. Consequently, the geometric diameter of the latter is substantially smaller than the aerodynamic diameter (relevant in the context of the VI). This aspect is not highlighted and it is not always clear which diameter is discussed. Consequently, a reader using the reported (aerodynamic?) diameters could be misled into applying them to geometric dust sizes.

Author's response: Aerodynamic diameter is used throughout the article. For clarity the adjective "aerodynamic" was added in several places. The fact, that virtual impactor characteristic depend on aerodynamic particle size was emphasized at the beginning of the Chapter 3.2.

Changes to the manuscript: Section 3.2, Line 369: "The concentration efficiency of the virtual impactor depends on the aerodynamic particle diameter. For that reason, an Aerodynamic Particle Sizer (APS, model 3321) was used both for analysis of aerodynamic particle size distribution during the campaign and virtual impactor characterization (Supplement S1)."

A constant value of the enhancement factor (EF) seems to be used. Yet EF is variable, as the authors' own data shows, and it will depend on particle aerodynamic size, hence the composition of the sample at any given time. This may be a major shortcoming, affecting the accuracy of the technique. Is it feasible to improve accuracy by using this dependence, perhaps taking advantage of on-line data? While this may not be possible with the current setup alone, the authors should comment on it and suggest potential solutions.

Author's response: The uncertainty introduced by using a constant value of EF for calculation of mineral dust concentration is 18% as noted in Chapter 3.7, page 14, line 578. Using APS for real-time determination of EF would reduce that uncertainty.

Changes to the manuscript: Section 3.7, Line 578: "This uncertainty can be reduced by using time-resolved measurements of EF or modifying the virtual impactor design to sharpen its response."

My general concern is about an unspoken shortcoming of the technique: it would fail if the dust and black carbon was internally mixed. As a warning to potential users, this should be highlighted, and the "climatology" of internal as opposed to external mixing described from known historical data.

Author's response: The proposed method is calibrated during the intensive campaign when MAC and EF are determined. Both parameters depend on the source region: EF is affected by the changes in size distribution which with time moves toward the smaller particles. MAC can be affected by the mineral dust composition, for example iron content and ionic state and also by black carbon content. The coagulation of mineral dust and black carbon is most intense at the source location because the process depends a lot on the aerosol concentration (Rodríguez et al., 2011). During transport the mineral dust and black carbon are diluted slowing the coagulation process. In both cases MAC of the mineral dust depends on the source region. The uncertainty of the method can be greatly reduced if the source region is determined from back-trajectory analysis and a specific MAC value is applied. This subject is being studied and will be reported in a separate article.

Changes to the manuscript: Section 3.7, Line 589: "Desert dust may mix with BC emissions and this is relevant especially at source regions, where concentrations are large enough for efficient coagulation between dust and BC to occur (Clarke et al., 2004; Rodríguez et al., 2011), with up to a third of carbonaceous particles internally mixed with mineral dust (Hand et al., 2010). The presence of BC on large dust particles will increase the MAC of the coarse fraction. The presence of BC on dust means, that for these source regions, larger MAC values will be used to convert the optical measurements into dust concentrations. BC present on dust particles contributes negligibly to the mass and the resulting increase in PM₁₀ concentrations is due to dust mass only. The increased MAC of these coagulated particles is also the relevant climate parameter, as dust and BC need to be taken into account together when estimating the direct radiative efficiency of such particles. To reduce the uncertainty resulting from different MAC values, a mineral dust source location can be determined using back-trajectory analysis and an appropriate MAC should be used for each source location."

Another absence is lack in the discussion (or introduction) of comparison of advantages and shortcomings with other methods, such as optical particle counting and aerodynamic sizing.

Author's response: Particle counting and sizing have not been included in discussion because these methods do not discriminate between mineral dust and other aerosol. Other qualitative and quantitative methods have been discussed in the Introduction. This discussion has been extended in line with the reviewers' comments.

Typos and corrections: Line 76: "allow for hourly" is written but "allow hourly" is meant.
Line 324: "Single" should be "single".

Author's response: The misspellings are corrected. Also the figure numbering was corrected.

References

Rodríguez, S., Alastuey, A., Alonso-Pérez, S., Querol, X., Cuevas, E., Abreu-Afonso, J., Viana, M., Pérez, N., Pandolfi, M., and de la Rosa, J.: Transport of desert dust mixed with North African industrial pollutants in the subtropical Saharan Air Layer, *Atmos. Chem. Phys.*, 11, 6663–6685, <https://doi.org/10.5194/acp-11-6663-2011>, 2011.

A new optical-based technique for real-time measurements of mineral dust concentration in PM₁₀ using a virtual impactor

5 Authors: Luka Drinovec¹, Jean Sciare², Iasonas Stavroulas², Spiros Bezantakos², Michael Pikridas², Florin Ungu²,
Chrysanthos Savvides³, Bojana Višić^{1,4}, Maja Remškar¹, Griša Močnik^{1,5}

¹Jozef Stefan Institute, Ljubljana, Slovenia

²Climate and Atmosphere Research Center, The Cyprus Institute, Nicosia, Cyprus

³Ministry of Labour, [Welfare](#) and Social Insurance, Department of Labour Inspection, Nicosia, Cyprus

⁴Institute of Physics Belgrade, University of Belgrade, Belgrade, Serbia

⁵Center for Atmospheric Research, University of Nova Gorica, Ajdovščina, Slovenia

Keywords: mineral dust, aerosol absorption, virtual impactor, PM₁₀

15 *Correspondence to:* luka.drinovec@ijs.si

20
25
30
35
40
45
Abstract. Atmospheric mineral dust influences Earth's radiative budget, cloud formation and lifetime, has adverse health effects, and affects the air quality through the increase of regulatory PM₁₀ concentrations, making strategic its real-time quantification in the atmosphere. Only few near-real-time techniques can discriminate dust aerosol in PM₁₀ samples and they are based on the dust chemical composition. The on-line determination of mineral dust using aerosol absorption photometers offers an interesting and competitive alternative, but remains a difficult task to achieve. This is particularly challenging when dust is mixed with black carbon, which features a much higher mass absorption cross-section. ~~We present here for the first time a highly time resolved on-line detection technique of dust absorption by coupling a high flow virtual impactor (VI) sampler that concentrates coarse particles with an aerosol absorption photometer (Aethalometer, model AE33). We build on previous work using filter photometers and present here for the first time a highly time resolved on-line technique for quantification of mineral dust concentration by coupling a high flow virtual impactor (VI) sampler that concentrates coarse particles with an aerosol absorption photometer (Aethalometer, model AE33).~~ The absorption of concentrated dust particles is obtained by subtracting the absorption of the submicron (PM₁) aerosol fraction from the absorption of the virtual impactor sample (VI-PM₁ method). This real-time method for detecting desert dust was tested in the field for a period of two months (April and May 2016) at a regional background site of Cyprus, in the Eastern Mediterranean. Several intense desert mineral dust events were observed during the field campaign with dust concentration in PM₁₀ up to 45 ~~μg~~ m⁻³. Mineral dust was present most of the time during the campaign with an average PM₁₀ of about 8 ~~μg~~ m⁻³. Mineral dust absorption was most prominent at short wavelengths, yielding an average mass absorption cross-section (MAC) of 0.24 ± 0.01 m² g⁻¹ at 370 nm and an absorption Ångström exponent of 1.41 ± 0.29. This MAC value can be used as site specific parameter for on-line determination of mineral dust concentration. The uncertainty of the proposed method is discussed by comparing and validating it with different methods.

1. Introduction

50 Atmospheric dust often dominates PM_{10} aerosol mass concentrations in many regions of the world, and is the second most abundant aerosol source at a global scale just after sea spray. Its lifetime in the atmosphere is similar to carbonaceous aerosols (Boucher et al., 2013). Dust particles modify the Earth's radiation balance as they absorb and scatter light, affecting regional climate and precipitation regimes. The net radiative effect of atmospheric dust depends on the interplay between the heating of the atmosphere, due to the increased absorption of sunlight, and cooling due to scattering of sunlight back into space leading to a direct radiative forcing of dust estimated around $-0.1 \pm 0.2 \text{ W m}^{-2}$ (Myhre et al., 2013). Dust deposits on snow and ice increase the ion content in snow and snow water (Greilinger et al., 2018) and they exert a warming influence after deposition (Di Mauro et al., 2015). Desert dust impacts our health and economy. Saharan dust events have been shown to increase morbidity and have negative influence on health mainly through respiratory and cardiovascular effects (Middleton et al., 2008; Perez et al., 2012). The health effects of mineral dust are being considered in the context of regulation (WHO, 2018). Dust soiling of photovoltaics is a significant factor in energy production and decreases their output by up to several percent (Mani and Pillai, 2010). Desert dust is a hazard for air and road transport, can cause electric fields detrimental for communication, and impacts water quality and plants, when deposited, resulting in great economic cost (Middleton, 2017), leading to the fictionalization due to its importance (Herbert, 1965).~~Dust deposits on snow and ice increase the ion content in snow and snow water (Greilinger et al., 2018) and they exert a warming influence after deposition (Di Mauro et al., 2015). Desert dust impacts industrial production to a degree that has been fictionalized (Herbert, 1965) and Saharan dust events have been shown to increase morbidity and have negative influence on health mainly through respiratory and cardiovascular effects (Middleton et al., 2008; Perez et al., 2012). The health effects of mineral dust are being considered in the context of regulation (WHO, 2018).~~

75 Dust particles are often transported from the Sahara over the Mediterranean and southern Europe and can contribute significantly to mass concentration of particles smaller than $10 \mu\text{m}$ in diameter - PM_{10} (Rodriguez et al., 2001; Vrekoussis et al., 2005). Mineral dust is considered as natural aerosol within the European Air Quality Directive (2008/50/EC) and, as such, can be subtracted from the daily (24h) PM_{10} reported by EU member states, potentially reducing the number of days with PM_{10} exceedances (European Commission, 2011).

80 Daily time resolution of the described method has been validated with the chemical composition and positive matrix factorization (PMF): the PM_{10} concentration above the daily regional background monthly 40th percentile has been shown to correlate well with aluminum (as a tracer of mineral dust), and the mineral dust factor from a PMF analysis (Viana et al., 2010).~~Daily time resolution of the described method has been validated with the chemical composition and positive matrix factorization (Viana et al., 2010).~~ Methods with higher temporal resolution have the potential to bring considerably more detail and information to the analysis of dust in PM_{10} . These methods capture the temporal variability dependent on the synoptic conditions more accurately; they allow the discrimination of long-range transported dust from locally resuspended one (by traffic as an important example); they provide considerably more detail to constrain chemistry-transport models; and can be used in real-time to inform the public and stakeholders and therefore improve adaptation measures. The higher time resolution requires use of novel and innovative approaches and instrumentation.

95 There are several sampling devices, which allow ~~for~~ hourly or sub-hourly sampling of ambient dust aerosols, such as the Streaker sampler, the DRUM (Davis Rotating-drum Unit for Monitoring) sampler (Bukowiecki et al., 2005; Visser et al., 2015) and the SEAS (Semi-continuous Elements in Aerosol Sampler) (Chen et al., 2016). Mass loadings of trace metals collected by these samplers can be analyzed with highly sensitive accelerator-based analytical techniques. However, a major drawback of these analyses is that they require a large commitment of analytical resources and time. Recent technical developments have ~~been developed for~~resulted in more precise, accurate and frequent measurement of ambient metal species, such as the XactTM 625 automated multi-metals analyzer (Fang et al., 2015; Jeong et al., 2016; Phillips-Smith et al., 2017; Cooper et al., 2010).

100 Dust scatters and absorbs light and its optical properties have been used in on-line measurements to derive the wavelength dependence of the single scattering albedo (SSA) (parameterized with the Ångström exponent) as the criterion to characterize Saharan dust events in the high Alpine region (Collaud Coen et al., 2004). The impact of Saharan dust events, showing increased absorption and scattering, was determined in the East Mediterranean (Vrekoussis et al., 2005) and the West Mediterranean (Pandolfi et al., 2011; Pandolfi et al.,

2014; Ealo et al., 2016). These measurements with high time resolution have shown that the optical properties can be used to identify dust events. Additionally, combining back-trajectory analysis and the SSA wavelength dependence, one can possibly detect local resuspension of dust, which impacts local air quality. However, these methods cannot determine the contribution of desert dust to PM_{10} concentrations in a quantitative manner.

110

~~These measurements with high time resolution have shown that the optical properties can be used to identify dust events but have not been able to determine the contribution of desert dust to PM_{10} concentrations in a quantitative manner based on the dust absorption.~~

115

Few studies have reported the potential of using dust aerosol absorption properties to infer their ambient concentrations in PM_{10} . These efforts started by using Aethalometers to determine the absorption coefficient attributed to iron compounds in dust, the determination of their mass absorption cross section, and the determination of black carbon and dust in the marine boundary layer (Fialho et al., 2005; Fialho et al., 2006; Fialho et al., 2014). The absorption of dust was due to iron compounds which were quantified using instrumental neutron activation analysis. Zhang et al. (2008) used thermal-optical reflection to measure the carbonaceous fraction and proton induced X-ray emission for elemental analysis, and again used iron as the dust tracer to separate the contributions of these two light-absorbing aerosol components. These publications systematically biased the absorption coefficients too high due to the assumption that the attenuation of light in the filter is due to non-filter-enhanced absorption, neglecting the enhancement due to the scattering in the filter matrix. Using different influence of iron-containing mineral dust and black carbon on SSA at different wavelengths and contrasting fine and coarse fractions, Derimian et al. (2008) quantified the iron concentrations in mineral dust. Lately, more sophisticated techniques using filter photometers were employed to determine the mineral dust absorption coefficients, mass absorption cross-sections and dust SSA. Caponi et al. (2017) used the multi-wavelength absorbance analyzer to determine the absorption coefficients at multiple wavelengths and obtain the absorption Ångström exponents and mass absorption cross-sections in a chamber study. The chamber study was also used to determine the filter enhancement in Aethalometers challenged with dust (Di Biagio et al., 2017) and then use these parameters to determine the optical properties as a function of iron content for different dust samples from all over the world (Di Biagio et al., 2019).

120

125

130

135

Additionally, quantitative determination of ambient concentration of mineral dust has been performed in the mixture of Saharan dust and carbonaceous matter in a wildfire plume (Schauer et al., 2016). These two may be internally mixed (Hand et al., 2010). The relationship between the columnar optical properties and the in-situ ones during dusty and dust-free days due to the mixing of the dust with the dominant local air pollution is challenging to interpret (Valenzuela et al., 2015).

140

Previous work has used two-component models to infer dust concentrations sampling ambient air on a filter in filter absorption photometers. However, the ~~The~~ determination of the optical absorption of pure mineral dust - when being externally mixed with black carbon - is more difficult because black carbon features a much higher mass absorption cross-section, obscuring the smaller contribution of dust to absorption. Enriching the aerosol coarse fraction, and hence increasing the contribution of weakly absorbing dust, may represent an innovative alternative way to increase dust aerosol absorption relative to black carbon.

145

We present here an improvement in real-time detection of mineral dust in ambient PM by concentrating the coarse particle fraction with a high-volume virtual impactor system similar to the one reported by Sioutas et al. (1994), and coupled with an aerosol absorption monitor (Aethalometer model AE33). We demonstrate its performance at a regional background site, frequently impacted by Saharan dust.

150

First the enhanced absorption of coarse particles is determined from the difference of absorption measured by Aethalometers with the virtual impactor and PM_{10} inlet, respectively. This parameter is divided by the enhancement factor calculated from the particle size distributions, yielding the absorption of coarse particles. The correlation between mineral dust absorption and reference mineral dust concentration provides us with the mass absorption cross-section of the mineral dust, which is then used to determine mineral dust concentration with high time resolution.

155

160

2. Materials and methods

2.1. Field campaign site description

165 Field validation took place at the Cyprus Atmospheric Observatory (CAO) between 1 April 2016 and 31 May
2016. This field campaign was organized as part of the European projects ACTRIS (Aerosols, Clouds and Trace
Gases Research Infrastructure) and BACCHUS (Impact of Biogenic versus Anthropogenic emissions on Clouds
and Climate; towards a Holistic UnderStanding). CAO is situated at a regional background site on the foothills of
170 mount Troodos (35.04N; 33.06E; 535 m a.s.l) in the centre of Cyprus, an island located in the Eastern
Mediterranean - Levantine basin. Lying in close proximity to the Middle-East/North Africa (MENA) region,
Cyprus is often influenced by air masses carrying mineral dust particles, originating from either the Saharan
Desert or the Middle East (Mamouri et al., 2013; Pikridas et al., 2018). During this field campaign, a large suite
of in-situ and remote sensing instrumentation was deployed at ground level and onboard Unmanned Aerial
Vehicles in order to better characterize the influence of desert dust on Ice Nuclei (Schrod et al., 2017; Marinou
et al., 2019), LIDAR retrieval of vertically-resolved *PM* (Mamali et al., 2018), and performance of miniaturized
175 light absorption sensors (Pikridas et al., 2019). More information on the climatology of air masses origin and
PM at the Cyprus Atmospheric Observatory can be found in Pikridas et al., 2018).

2.2. Instrumentation

180

Real-time aerosol absorption of the dust-containing coarse fraction was determined by subtracting aerosol absorption of black carbon-containing submicron aerosols from the absorption of the concentrated coarse aerosols from the outlet of a virtual impactor (VI). A detailed description of this instrumental set-up as well as complementary aerosol instrument is provided in the following.

185

2.2.1. Virtual Impactor design

190

Based on a design similar to the one reported by Sioutas et al. (1994), our virtual impactor is sampling ambient air (TSP) at a total flow rate of 100 l min^{-1} . The major flow ($F_{in} = 98 \text{ l min}^{-1}$) is carried out of the VI by a large capacity pump while the coarse particles are inertially impacted (enriched) into the minor flow ($F_{out} = 2 \text{ l min}^{-1}$) of the VI connected to the absorption photometer. The enrichment of coarse particles in the minor flow is a function of the ratio of the two (major/minor) flows; its efficiency depends also on the design and manufacturing of the VI. For that reason, the VI was thoroughly tested and characterized in the lab in order to estimate the concentration ~~enhancement efficiency (CE)-factor~~ of coarse particles as a function of aerodynamic particle size (using NIST polystyrene-latex (PSL) spheres with nominal aerodynamic sizes from 0.7 to $10 \text{ }\mu\text{m}$) and two different flow rate ratios (19 and 50, respectively). The laboratory characterisation of the VI is described in the Supplement S1 while the methodology used to reconstruct the size distribution of concentrated coarse particles (in the minor flow F_{out}) is presented in section 3.1.

195

200

205

210

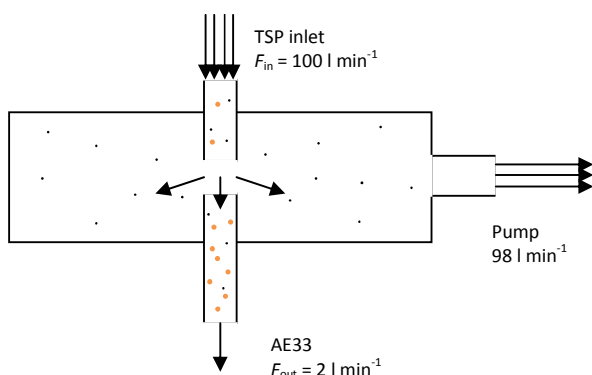


Figure 1. Principle of the Virtual Impactor (VI) operation.

215

2.2.2. Aerosol absorption and light scattering coefficients

220

Three Aethalometers model AE33 (Magee Scientific, USA) were used during the field campaign with different inlet setups: one sampling through a PM1 sharp-cut cyclone (BGI Inc., Model SCC 1.197), one sampling through a custom-made total suspended particles (TSP) inlet and a third one sampling through the VI described above (Section 2.2.1). The first two instruments (with PM1 and TSP) were sampling at a 5 l min^{-1} flow rate, while the third was sampling through the VI at a 2 l min^{-1} flow rate. This flow rate of 2 l min^{-1} was selected so as to increase concentration ~~enhancement efficiency (CE)-factor~~ of the VI and consequently increase the absorption signal of dust aerosols.

225

The Aethalometer AE33 measures attenuation of light by two samples collected at different flow rates. This results in two sample spots that feature different attenuation values. The measurement of light transport through the sample-laden filter is non-linear and the measurements using two sample spots allow the on-line compensation of the nonlinearity of the black carbon measurement (Drinovec et al., 2015). Given that the on-line filter loading compensation was not working efficiently for the AE33 coupled with the virtual impactor (see section 3.3, below), the obtained data was compensated using fixed filter loading compensation parameter k values as described in the Supplement S2.

230

Absorption coefficient (b_{abs}) was calculated from the attenuation coefficient (b_{atn}) using the value of the multiple scattering parameter C of 2.657:

235

$$b_{\text{abs}} = \frac{b_{\text{atn}}}{C} \quad (1)$$

240

The calculation of the absorption coefficient was updated from the Drinovec et al. (2015) following the WMO guideline (WMO, 2016): we updated the value of the filter multiple-scattering parameter C . The multiple-scattering parameter C in Drinovec et al. (2015) determined the AE33 filter C values relative to the value of the quartz filter, used in older AE31 instruments. This AE31 value was assumed to be 2.14 (Weingartner et al., 2003), but it was later recommended to use an AE31 value of 3.5 (WMO, 2016). The parameter $C = 1.57$ used for the AE33 filter (Drinovec et al., 2015) was renormalized using the same factor resulting in a new value $C = 2.57$. The mass absorption cross-section σ_{air} for black carbon was adjusted in the inverse manner to obtain the same BC. The new mass absorption cross section for black carbon σ_{air} at 880 nm is now $4.74 \text{ m}^2 \text{ g}^{-1}$ instead of $7.77 \text{ m}^2 \text{ g}^{-1}$.

245

250

This value was derived from the value obtained for quartz filter: 3.5 (WMO, 2016) instead of 2.14 used previously (Weingartner et al., 2003) and adjusted for the AE33 filter (Drinovec et al., 2015) to 2.6 instead of 1.57. The σ_{air} value for black carbon was adjusted in the inverse manner to obtain the same BC values; new mass absorption cross section for BC σ_{air} at 880 nm is now $4.74 \text{ m}^2 \text{ g}^{-1}$ instead of $7.77 \text{ m}^2 \text{ g}^{-1}$.

$$BC = \frac{b_{\text{abs}}}{\sigma_{\text{air}}} = \frac{b_{\text{atn}}}{C \cdot \sigma_{\text{air}}} \quad (2)$$

255

The Aethalometers were intercompared in the laboratory before the campaign. The correlation slope for 1 minute resolution data differed less than 4% between the instruments with $R^2 = 0.996$. The analysis of the actual uncertainty of Aethalometer measurements during the campaign is presented in the Supplement S3.

260

Total scattering and back-scattering coefficients (b_{scat} & b_{bscat}) of the ambient (TSP) aerosol were monitored continuously using a three-wavelength (450, 550 and 700 nm) integrated nephelometer (TSI Inc., model 3563; Anderson and Ogren, 1998). The nephelometer was sampling through a vertical, straight sampling line, coupled with a TSP inlet, a Nafion dryer, and measuring at 1-minute time resolution. Calibration was conducted using CO_2 as a high, and zero air as a low span gas prior to the field campaign. This nephelometer went through a successful inter-comparison exercise at the European Center for Aerosol Calibration (ECAC-report-IN-2015-1-5, 2016) ahead of the instrument's field deployment. Nevertheless, due to miscalibration of the green channel, 550 nm measurements were excluded from the analysis. Single scattering albedo (SSA) was calculated at 450 and 700 nm using the total scattering coefficient from nephelometer and absorption coefficient obtained from AE33 by linear interpolation of absorption coefficients from adjacent wavelength pairs. Single scattering albedo Ångström exponent (SSAAE) was calculated from $SSA_{450 \text{ nm}}$ and $SSA_{700 \text{ nm}}$.

265

270

2.2.3. Other in-situ aerosol instrumentation

Dried particle number size distributions (PNSDs) were measured using a TSI Inc. Aerodynamic Particle Sizer (APS, model 3321). The APS measures PNSDs in the 0.5 - 20 μm aerodynamic diameter size range at a 5-minute temporal resolution. The APS was sampling at a total flow rate of 5 l min^{-1} through a straight vertical sampling line, a Nafion dryer, and a TSP inlet, identical to the nephelometer. Aerosol mass concentration for fine ($PM_{2.5}$) and coarse aerosols ($PM_{10-2.5}$) was measured using a Continuous Dichotomous Ambient Particulate Monitor (Thermo Scientific, 1405-DF TEOM-FDMS system) deployed at the Agia Marina Xyliatou EMEP station, collocated with CAO, at a 1-hour temporal resolution (see more at Pikridas et al., 2019).

275

280

2.3. Filter sampling and analysis

2.3.1 Filter sampling

Aerosol samples were collected during the field campaign at a flow rate of $2.3 \text{ m}^3 \text{ h}^{-1}$ on pre-weighed filters (Pall Tissuquartz 2500 QAT-UP) using two autonomous filter samplers (Leckel SEQ 47/50) for determination of mass concentration ($PM_{2.5}$ and PM_{10} , respectively) with 24-h time resolution from midnight to midnight according to local standard time. Particle mass concentration ($PM_{2.5}$ and PM_{10}) on the filter substrates was

285

determined gravimetrically before and after the sampling, under constant conditions dictated by protocol EN12341 with the use of a 6 digits precision analytical balance (Mettler Toledo, Model XP26C). According to that protocol filters were subjected to 45-50% relative humidity at $20 \pm 1^{\circ}\text{C}$ for 48 hours.

290

2.3.2 Aerosol chemical mass closure

Filter samples were subsequently analyzed for major ions by ion chromatography (Thermo, Model ICS5000) following the protocol reported in Sciare et al. (2011) and complying with the European committee for standardization for the measurement of anions and cations in PM_{2.5} (EN 16913:2017) and elemental carbon concentration (EC) and organic carbon concentration (OC) with a Sunset Lab Instrument, the EUSAAR_2 thermo-optical protocol (Cavalli et al., 2010) and complying with the European committee for standardization (EN 16909:2017). Quality of ion measurements is checked at the bi-annual intercomparison studies performed in the framework of the EMEP and WMO networks while quality of EC/OC measurements is confirmed on annual basis in the framework of ACTRIS network.

300

Estimation of dust in $PM_{2.5}$ and PM_{10} was performed following the methodology proposed by Sciare et al. (2005) for a regional background (Crete Island) located in the Eastern Mediterranean assuming a constant Calcium-to-dust ratio of 0.12. Reconstruction of PM from chemical analyses versus PM from gravimetry is reported in Supplement S6 and shows very good correlation ($R^2 = 0.99$) and slope close to one, supporting the consistency and robustness of our calculation of mineral dust in PM .

305

2.3.3 Trace metal analysis using inductively coupled plasma mass spectrometry (ICP-MS)

An acid microwave digestion procedure was applied to the PM_{10} filters followed by inductively coupled plasma mass spectrometry (ICP-MS, Thermo Electron X Series) to measure metal concentrations of Al, V, Cr, Mn, Fe, Ni, Cu, Zn, Cd, and Pb, following the procedure from Poulakis et al. (2015).

310

2.3.4 Scanning electron microscopy – energy dispersive X-ray (SEM-EDX) analysis

Scanning electron microscopy measurements were performed at Jožef Stefan Institute using SEM model Supra 35 VP (Carl Zeiss, Germany). Measurements were performed on punches of PM₁₀ filters that were attached to the sample holder through a double-sided carbon tape. The filters were previously sputter-coated with a thin gold film (with Au nanoparticle approximate size of 10 nm) using an SCD 005 cool sputter coater (BAL-TEC GmbH, Leica Microsystems, Wetzlar, Germany). The microscope was equipped with the energy dispersive spectroscopy module (EDX, Oxford INCA 400, Oxford Instruments Analytical, UK), which was operated at an accelerating voltage of 20 kV.

315

320

2.4. Data coverage

The measurement campaign took place in April and May 2016. Due to technical reasons not all of the instruments were running throughout the campaign (Table 1). This limited some of the analysis to a shorter time periods with most of the data available between 14 April and 6 May.

325

Table 1. Data coverage for on-line instrumentation and filter sampling.

Instrument	Available data
AE33	4 Apr 2016 - 31 May 2016
VI	14 Apr 2016 - 6 May 2016
TEOM-FDMS	1 Apr 2016 - 31 May 2016
Nephelometer	14 Apr 2016 - 31 May 2016
APS	1 Apr 2016 - 30 Apr 2016
24h filter samples	1 Apr 2016 - 31 May 2016

330

3. Results and discussion

335 The absorption of the fine aerosol fraction, dominated by black carbon, is usually much larger compared to the
absorption in the coarse fraction, which contains mineral dust. In other words, $b_{abs,TSP}$ is expected to be close to
 $b_{abs,PM_{10}}$. Subtracting these two signals close in absolute values (but with large uncertainties), would result in a
340 close-to-zero number associated with a large measurement error. The proposed VI method takes advantage of
the concentration of coarse particles using a virtual impactor to enhance the coarse fraction in the sample, and
subtracts the absorption of the fine fraction (as the VI sample contains the same amount of fine fraction as an
ambient sample). To calculate the absorption of the coarse fraction, the concentration efficiency of the virtual
impactor must be taken into account.

345 The methodology to derive real-time concentration of dust in PM_{10} is presented as per the follow: the
robustness of the system (VI+AE33) is tested first in the field for a period of 1 month in Section 3.1. The
enhancement factor (EF) downstream of the virtual impactor is calculated in Section 3.2. Real-time absorption
of ambient dust aerosols is calculated in section 3.3. It is corrected for 1) the influence of bBlack cCarbon
measured by a co-located Aethalometer AE33 equipped with PM_{10} inlet, and 2) the eEnhancement fFactor
of the VI. Real-time dust concentration of PM_{10} (Section 3.4) is then derived by dividing the absorption of dust
aerosols calculated in section 3.3 with a mMass aAbsorption cCross-section (MAC) for dust calculated using
350 filter-based chemical analyses.

3.1. Field campaign overview

355 Optical, physical, and size-resolved chemical properties of ambient aerosols at the Cyprus Atmospheric
Observatory were characterised continuously in April and May 2016 using several online and offline methods
as illustrated in Figure 2. During the campaign a total of four intense events (16 and 26 April, 1 and 15 May
2016) were detected with increased PM concentration of the coarse fraction concurrent with increase of the
light scattering coefficient, but no correlation with black carbon concentration (Figure 2). By combining light
absorption and scattering measurements it is possible to identify the mineral dust events as the periods during
360 which the single scattering albedo Ångström exponent ($SSAAE$) becomes negative, indicating the presence of
mineral dust (Collaud Cohen et al., 2004).

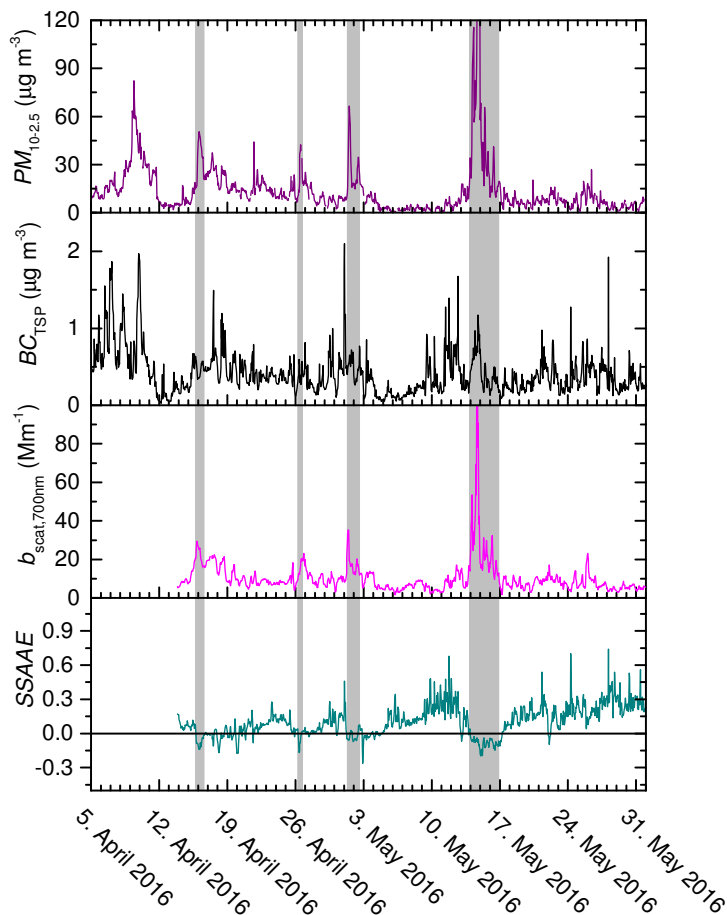


Figure 2. Time series of the mass concentration of coarse particles ($PM_{10-2.5}$) obtained by TEOM-FDMS, black carbon concentration (BC) for total suspended particles (TSP) obtained by Aethalometer AE33, the light scattering coefficient at 700 nm obtained by nephelometer and Single-single scattering albedo Ångström exponent (SSAAE). The four periods with negative SSAAE during the campaign are shadowed.

365

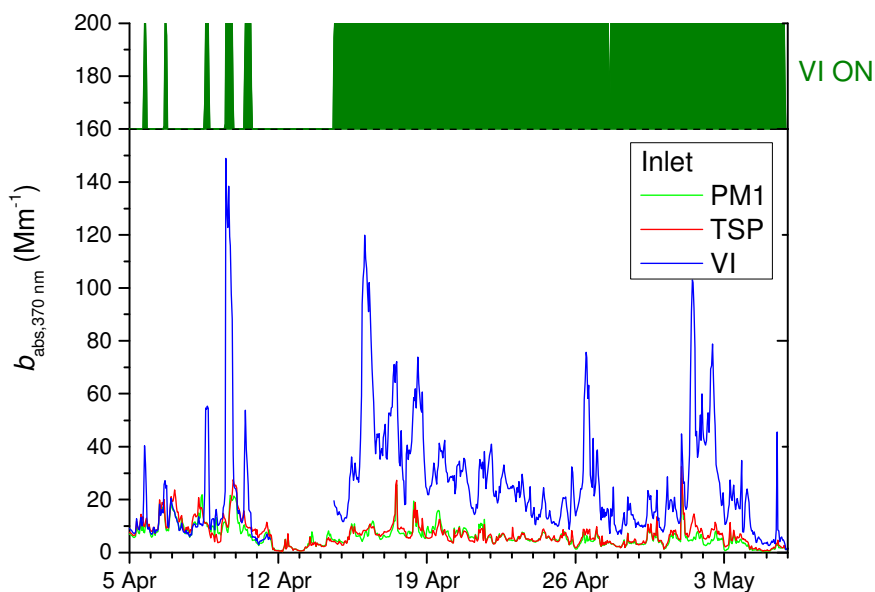
Figure 3 reports continuous measurements of aerosol absorption during the field campaign for three different aerosol size fractions that were achieved using different inlets for three Aethalometers AE33 running in parallel: 1) a PM_{10} ; 2) a total suspended particle (TSP), and 3) a virtual impactor (VI). During the first days of the campaign, the VI was operated manually for several periods of few hours in order to perform several tests related to the collection and light absorption detection of the coarse fraction. The VI was set ON continuously from 14th April till 6th May. Given the strong sensitivity of dust aerosol absorption in the UV range compared to black carbon (see Section 3.3), the 370 nm channel was selected here to compare aerosol absorption measurements from the three Aethalometers.

370

375

As shown in Figure 3 the absorption in TSP is closely related to the one of PM_{10} . The differences are inside the measurement uncertainty of the Aethalometers (Supplement S3). On contrary, the absorption measured when the virtual impactor was ON shows very high values and very poor correlation with the other absorption measurements. During the periods when the VI pump was not operating, the aerosol absorption agrees well with the one using the TSP showing that the enhancement of aerosol absorption is entirely related to the enhancement of the coarse fraction.

380



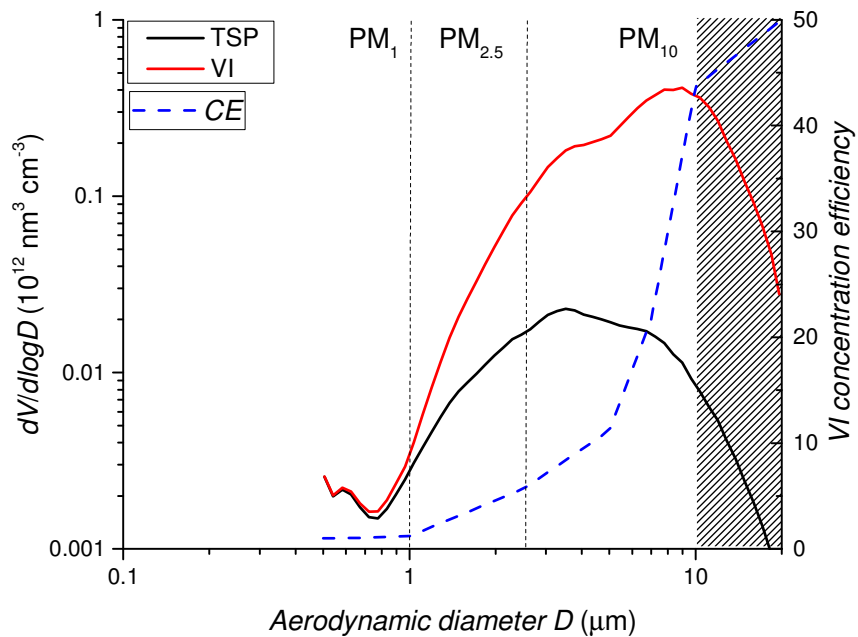
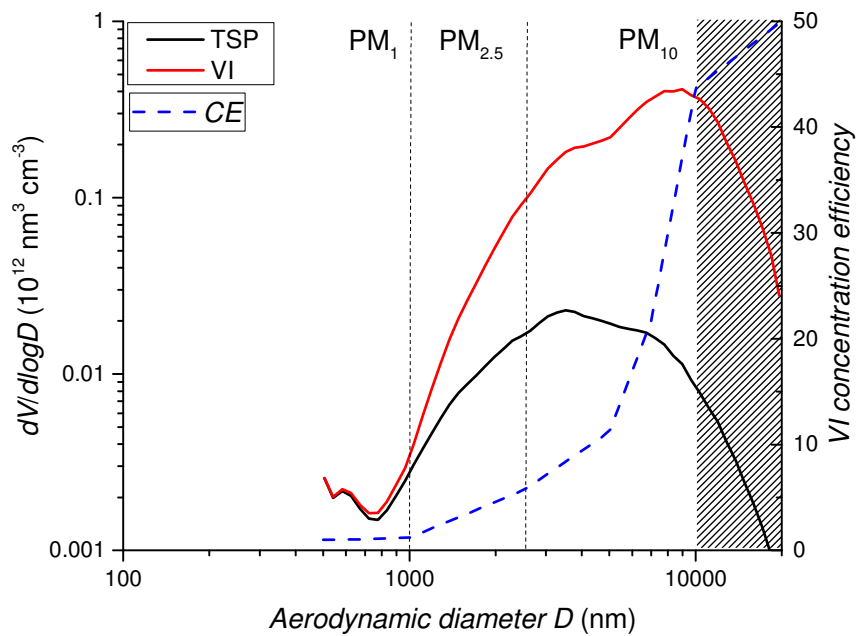
385 Figure 3. Time series of the aerosol absorption coefficient at 370 nm for three Aethalometers AE33 running in parallel and equipped with different inlets: PM₁, total suspended particle (TSP) and virtual impactor (VI). The periods when VI was operating are marked in green (VI=ON).

3.2. Experimental characterization of the enhancement factor of coarse particles using the virtual impactor

390 ~~The concentration efficiency of the virtual impactor depends on the aerodynamic particle diameter. For that reason an Aerodynamic Particle Sizer (APS, model 3321) was used both for analysis of aerodynamic particle size distribution during the campaign and virtual impactor characterization (Supplement S1). The performance of the virtual impactor was characterised during the laboratory campaign (Supplement S1).~~ The maximum concentration efficiency (CE) was obtained for F_{in}/F_{out} ratio of 50 (Table S1). ~~Using the minimum sample flow of AE33 of 2 lpm and maximum flow of the virtual impactor pump we obtained the maximum~~ Therefore, a similar F_{in}/F_{out} ratio of 50 ~~was chosen during the field deployment with F_{in} of 100 l min⁻¹ and F_{out} of 2 l min⁻¹, respectively.~~ As shown in Table S1 for F_{in}/F_{out} ratio of 50, the concentration efficiency (CE) of aerosols with aerodynamic diameters of 1 μ m and below is close to unity. This result is expected for a virtual impactor which principle is based on the concentration of large aerosols. Consequently, the black carbon fraction ~~is~~ mainly located in the submicron mode ~~is~~ is not enriched in the VI. On contrary, dust aerosols - mostly located in the coarse aerosol fraction (above 1 μ m diameter) are concentrated efficiently by the virtual impactor (Figure 4).

395

400



405 Figure 4. Average aerodynamic volume size distribution spectrum measured by APS between 1 April 2016 - 30 April 2016 (black line) and the predicted spectrum of aerosol concentrated using the virtual impactor (red line). Blue line represents the virtual impactor concentration efficiency measured in laboratory (Supplement S1). Shaded area denotes the particles larger than 10 μm .

410 The enhancement factor (EF) of the VI is defined as a multiplication factor that reflects the enrichment of the coarse fraction downstream of the VI. EF was determined experimentally during the field test using the Aerodynamic Particle Sizer (APS) to derive both the volume concentration of the unperturbed sample (V) and volume concentration enhanced using a virtual impactor (V_{VI}):

415
$$V = \int \left(\frac{dV}{d \log D} \right) * d \log D \quad , \quad (3)$$

$$V_{VI} = \int \left(\frac{dV}{d \log D} \right) * CE * d \log D \quad , \quad (4)$$

420 | where D is the particle aerodynamic diameter and CE the collection-concentration efficiency of the VI as characterized in supplement S1. The enhancement factor is then calculated as:

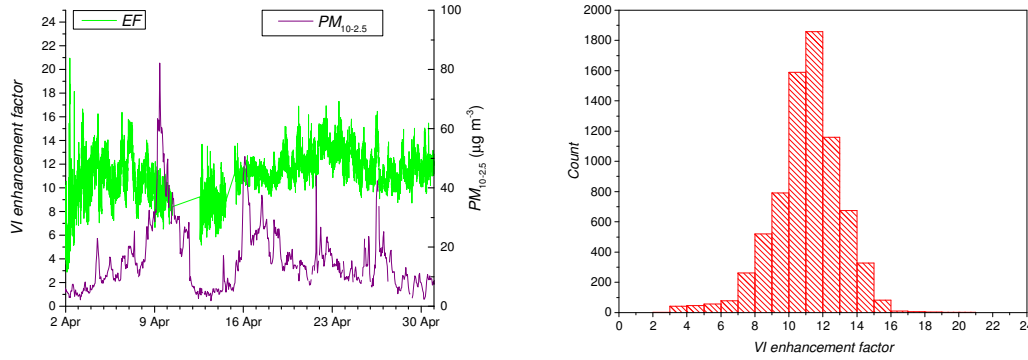
$$EF = \frac{V_{VI}}{V} \quad . \quad (5)$$

425 The average aerosol volume concentration size spectrum obtained during the campaign by the APS is presented in Figure 4 (black line), along with the spectrum calculated for the virtual impactor (red line), using the concentration efficiency determined during the laboratory campaign (Table S1). For ambient aerosol we observe a mode around 3.5 μm . Because the virtual impactor is more efficient towards larger particles, the ambient volume size distribution is not reproduced downstream of the VI, which shows a maximum around 9 μm . The collection efficiency of particles larger than 10 μm in the Aethalometer AE33 downstream the VI is
 430 expected to be rather low due to losses in tubing and sample lines inside the Aethalometer. Overall, the uncertainty associated with the enhancement factor remains difficult to assess in the aerosol range close to 10 μm diameter which particles are usually difficult to collect in a quantitative way.

435 The enhancement factor of the VI defined in Eq. 5 depends on the ambient aerosol volume size distribution measured by the APS, which changes over time. Figure 5 reports the temporal variation of EF during the field campaign at 5 min time resolution. There are time intervals with stable EF of approximately 9 (11 April 2016 - 13 April 2016), also we can observe some peaks with EF as high as 16. For the PM_{10} - PM_1 particles we obtained a campaign average VI enhancement factor:

440

$$EF = 11 \pm 2.$$



a)

b)

445

Figure 5. Time series of the virtual impactor enhancement factor calculated from aerodynamic size distributions measured by APS (a) for the PM_{10} aerosol fraction. The enhancement factor frequency distribution is shown on the right (b).

450 3.3. Calculation of the absorption coefficient of coarse particles

The principle of the virtual impactor operation allows for concentration of the coarse particles while the fine particles remain present at the same amount as in the ambient air. To determine the absorption induced by ambient mineral dust, we need to subtract the fine particle absorption signal (dominated by black carbon) from the total virtual impactor absorption and normalize by the enhancement factor, following the equation:

455

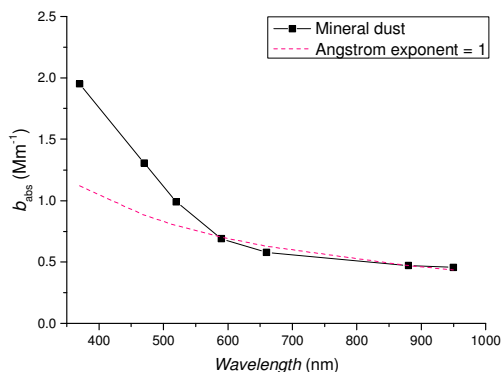
$$b_{abs, \text{mineral dust } PM_{10-1}} = \frac{b_{abs, VI} - b_{abs, PM_1}}{EF}, \quad (6)$$

460 where $b_{abs, PM_{10-1} \text{ mineral dust}}$, $b_{abs, VI}$ and b_{abs, PM_1} represent absorption coefficients of dust in ambient conditions, aerosols downstream of the virtual impactor and submicron aerosols, respectively. Because absorption of PM_1 fraction is dominated by black carbon, it is essential to compensate absorption data for the filter loading effect (Drinovec et al., 2017). If the compensation parameter is wrong by 0.005 this can result in over- or under-estimation of b_{abs} by up to 60% at 370 nm and by 25% at 950 nm. For the Aethalometer with the PM_1 inlet, the absorption data is sufficiently compensated by the built-in dual-spot algorithm. For the Aethalometer connected to the virtual impactor, the method was not able to measure accurately the loading effect due to the presence of coarse particles (Supplement S2). The main reason for this behaviour lies in the fact that a single particle (deposited on one of the two spots) potentially causes significant absorption only in one of the two measurement spots. This requires an application of off-line compensation using fixed values of the compensation parameters (Supplement S2).

470

The absorption induced by dust (Eq. 6) during the field campaign was calculated for each of the 7 wavelengths of the Aethalometer AE33 and averaged, as shown in Figure 6. The spectral dependence of absorption by mineral dust shows an increase at shorter wavelengths, significantly deviating from the Ångström exponent of 1. The best discrimination between the mineral dust particles and black carbon is achieved at the lowest wavelength 370 nm, which is the wavelength that has been selected in our procedure to derive the absorption and the atmospheric concentration of mineral dust.

475



480 Figure 6. Averaged absorption coefficient during the campaign for ambient dust (as calculated in Eq. 6) in the coarse fraction of aerosols as calculated from the difference of the absorption coefficients measured with a virtual impactor and a PM₁ inlet, and divided by the average enhancement factor (black line). The dotted red line shows a theoretical curve with Ångström exponent of 1, extrapolated from measurements at 880 nm.

485 Campaign averages show the mean value for absorption at 370 nm being higher for TSP compared to PM₁ inlet (Table 2). The absorption signal reported in this table for the AE33 behind the VI is more than a factor of 4 higher compared to AE33 with the PM₁ inlet and is due to the concentrated mineral dust in the coarse fraction. The average absorption coefficient of ambient dust as calculated using Eq. 6 was $2.0 \pm 2.1 \text{ Mm}^{-1}$. Similarly to absorption, AAE shows higher value for TSP compared to PM₁ inlet, as the mineral dust in the coarse fraction increases absorption in UV & blue part of the spectrum. As expected there is high variability both for absorption and AAE during the campaign. The average difference between absorption for TSP and PM1 inlets is lower than expected from the (VI-PM1)/2 absorption value. This is a consequence of high measurement uncertainty of up to 18% during the campaign (as estimated comparing Aethalometers with different inlets, Supplement S3). Mineral dust absorption calculated from the difference between $b_{\text{abs},370\text{nm}}$ for TSP and PM1 of 0.6 Mm^{-1} has an uncertainty 2.1 Mm^{-1} . ~~, but within the measurement variation and uncertainty the $b_{\text{abs},370\text{nm}}$ measurements were affected by the uncertainty up to 18% during the campaign (as estimated comparing Aethalometers with different inlets, Supplement S3).~~

495
500 Table 2. Average absorption coefficient at 370 nm, the absorption Ångström exponent (AAE) and their variation **between** during the campaign (15 April 2016 and 6 May 2016). AAEs were calculated as averages of one hour values for the wavelength pair of 370 and 950 nm.

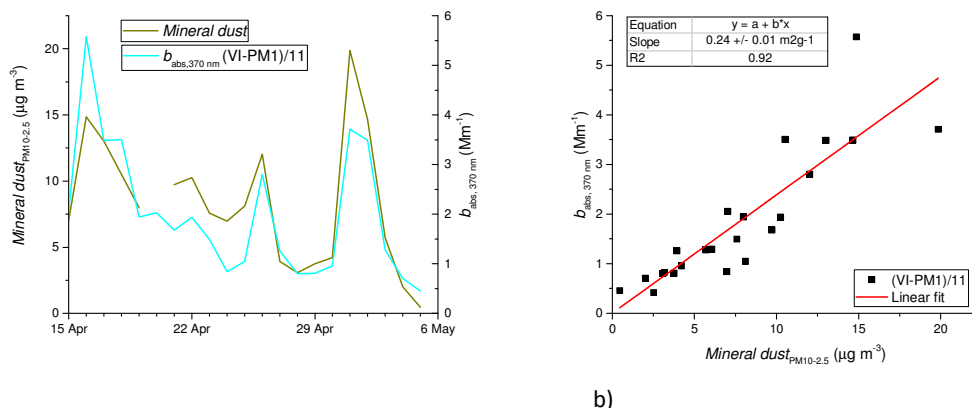
Sample	$b_{\text{abs},370\text{nm}} (\text{Mm}^{-1})$	AAE
PM1	5.6 ± 3.3	1.22 ± 0.16
TSP	6.1 ± 3.4	1.30 ± 0.18
VI	27.6 ± 20.1	1.38 ± 0.25
VI-PM1	22.0 ± 23.4	1.41 ± 0.29
(VI-PM1)/11	2.0 ± 2.1	1.41 ± 0.29

3.4. Determination of mineral dust mass absorption cross-section

505

For the determination of the mineral dust mass absorption cross-section, we need to establish the mineral dust concentration in our samples. For this purpose, we performed mass closure on 24-hour PM₁₀ and PM_{2.5} filter samples (see Supplement S6). Mineral dust concentration was determined from calcium concentration, assuming 12% Ca in mineral dust. Since the virtual impactor concentrates larger particles with higher efficiency (this is where we expect to have the largest contribution of mineral dust), we used the coarse fraction PM_{10-2.5} for the calibration (Figure 87).

510



a)

b)

515

Figure 87. The time-series (a) and the correlation (b) between the absorption coefficient of coarse particles obtained using VI-PM1 method versus mineral dust concentration in the coarse fraction.

520

The correlation between mineral dust absorption and filter measurements is very good with R^2 of 0.92 showing good agreement between the methods. The mineral dust mass absorption cross-section was obtained from the regression between mineral dust mass and the coarse fraction absorption coefficient at 370 nm:

$$MAC_{\text{mineral dust},370\text{nm}} = 0.24 \pm 0.01 \text{ m}^2 \text{ g}^{-1}.$$

525

This MAC value, obtained with 24-h time resolution, allows us to calculate mineral dust concentrations with the high time resolution of the absorption measurements:

$$\text{Mineral dust}_{\text{PM}_{10-2.5}} = \frac{(b_{\text{abs},370\text{nm,VI}} - b_{\text{abs},370\text{nm,PM1}})}{EF \cdot MAC_{\text{mineral dust},370\text{ nm}}} \quad (7)$$

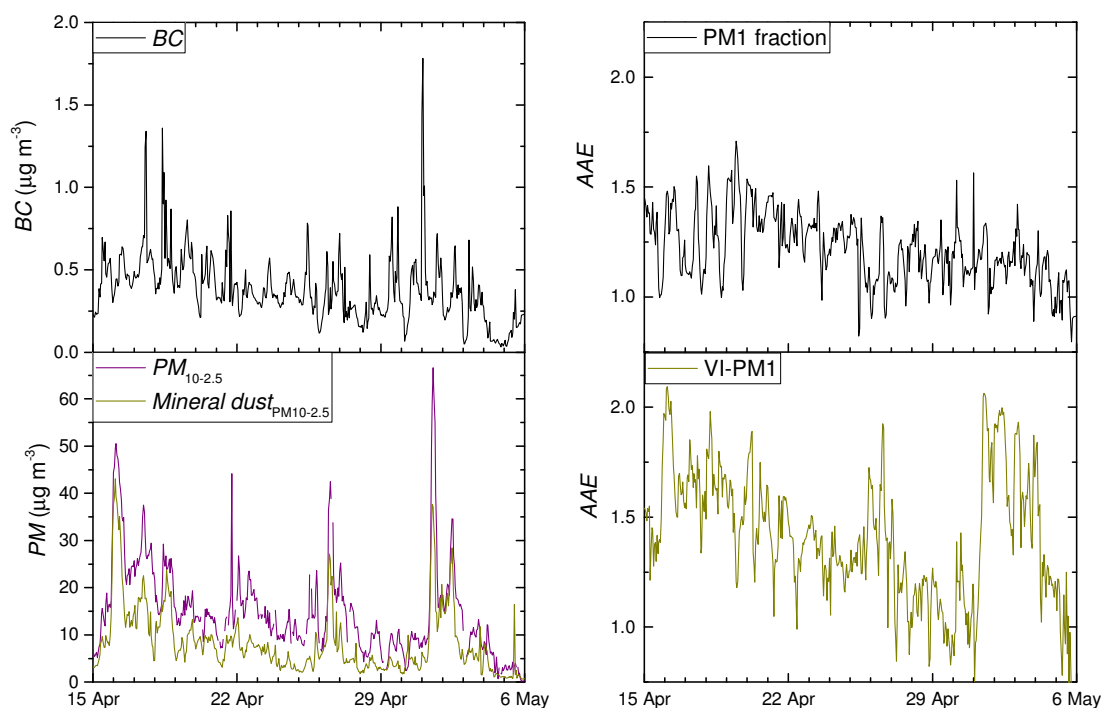
530

The concentration of coarse particles and its composition show a huge variability during the campaign (Figure 9a): the average mineral dust concentration was $8.1 \mu\text{g m}^{-3}$ with peaks up to $45 \mu\text{g m}^{-3}$. On average, mineral dust represented about one half of the coarse fraction. The average BC was much lower at $0.39 \mu\text{g m}^{-3}$. Due to its much higher mass absorption cross-section ($MAC_{\text{BC},370\text{nm}} = 11.2 \text{ m}^2 \text{ g}^{-1}$; 47 times higher compared to mineral dust), the absorption of black carbon dominated the aerosol absorption in Cyprus during the campaign and mineral dust absorption could not be detected directly. Using the virtual impactor allows us to concentrate the dust and measure its absorption coefficient and determine its mass absorption cross-section with a low uncertainty.

535

540

The Ångström exponent of the fine fraction oscillates between 1 and 1.5 (Figure 9b). The lower values correspond to BC peaks, originating from local traffic and other efficient combustion sources. The higher values are a mixture of mineral dust and local pollution. The Ångström exponent of the coarse fraction reaches value of 2.1 during intense mineral dust periods. After these events the AAE value drops slowly and reaches a value of 1.2 during the period with low presence of mineral dust (around 27 April 2019 - 1 May 2019).



545

a)

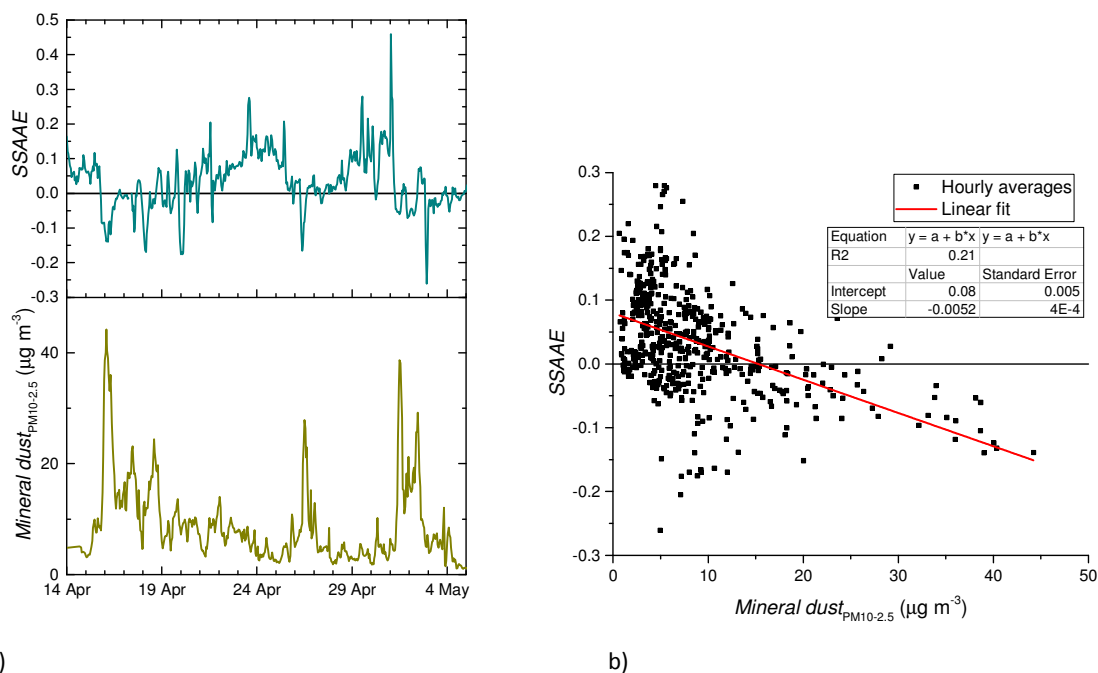
b)

Figure 9. Time series of BC in fine fraction and mineral dust determined using VI-PM1 method (a) and Ångström exponent for fine and coarse fraction of the aerosol (b).

550

The knowledge of the virtual impactor enhancement factor allowed us to calculate the average MAC for mineral dust during the Cyprus campaign. Reportedly, its value depends mostly on the absorption of iron oxides (Sokolik and Toon, 1999; Alfaro et al., 2003; Fialho et al., 2005; Fialho et al., 2006; Fialho et al., 2014; Caponi et al., 2017; Di Biagio et al., 2019). During the campaign we obtained 1.9% iron in PM_{10} . If we take into account that mineral dust represented about one half of PM_{10} (Supplement S6), we get a good agreement with iron concentrations measured for mineral dust from Middle East of 3.15% - 3.5% (Linke et al., 2006), 3.8% - 5% (Caponi et al., 2017) and Sahara of 3.6% - 6.6% (Caponi et al., 2017). Surprisingly our $MAC_{\text{Mineral dust}, 370\text{nm}} = 0.24 \text{ m}^2 \text{ g}^{-1}$ is much larger compared to mineral dust from Saudi Arabia of $0.09 \text{ m}^2 \text{ g}^{-1}$, Libya of $0.089 \text{ m}^2 \text{ g}^{-1}$ and Algeria of $0.099 \text{ m}^2 \text{ g}^{-1}$ (Caponi et al., 2017) or North-Eastern Africa of $0.099 \text{ m}^2 \text{ g}^{-1}$ (Fialho et al., 2006). Higher MAC goes along with the low Ångström exponent value of 2.1 obtained for the fresh mineral dust reaching Cyprus. This value is lower than AAE of 2.8 - 4.1 reported for Middle East (2.8 - 4.1) and Sahara (2.5 - 3.2) by Caponi et al. (2017) or 2.9-4 for North-Eastern Africa (Fialho et al., 2005; Fialho et al., 2006). Differences in MAC values and the Ångström exponent can be an indicator that the coarse fraction of mineral dust is contaminated with black carbon, with the mixing occurring in or close to the source regions much earlier than mineral dust reached Cyprus. Simulations show that black carbon stuck to the mineral dust particles can severely change its optical properties, but the effect depends on the particle size (Scarnato et al., 2015). Because of the differences in dust mineral composition and contamination with BC we expect MAC to be source region specific.

565



570

a) b) **Figure 10. Time-series (a) and correlation (b) of the single scattering albedo Ångström exponent (SSAAE) and mineral dust concentration.**

575

The determination of the mineral dust concentration was tested using the Collaud Coen et al. (2004) method for the qualitative determination of Saharan dust events. As expected the peaks in mineral dust concentration correspond to the periods featuring negative values of single scattering albedo Ångström exponent. It is shown (Figure 10) that SSAAE becomes negative when the mineral concentration becomes larger than $15 \mu\text{g m}^{-3}$. The correlation between the mineral dust (determined from the chemical composition, notably calcium ions) and SSAAE is not perfect because of the contribution to scattering from other aerosol components (organics, sulphates, sulphates ...) which amount to about one half of the aerosol mass, and the absorption of organics. While the SSAAE method provides an identification of dust events, the VI-PM1 method allows for the quantitative determination of mineral dust - even at high black carbon concentrations in the fine fraction.

580

585

3.7. Uncertainty of the VI-PM1 method for the determination of mineral dust concentrations in PM_{10}

The uncertainty in the determination of mineral dust concentration using VI-PM1 method arises from the measurement uncertainties, variability of optical and chemical properties of mineral dust and potential systematic biases of the method itself. Because Since the VI-PM1 method is calibrated using mineral dust in the coarse fraction only, 6% lower values compared to total mineral dust in PM_{10} are reported. This bias can be avoided by using a correction factor.

590

595

The uncertainty of 10% in the determination of the attenuation coefficient at 880 nm by the Aethalometer AE33 was reported (Drinovec et al., 2015). The performance of the Aethalometers during this campaign was investigated by comparing signal from the instruments with TSP and PM_1 inlets. The variation not related to the presence of mineral dust was used to determine measurement uncertainty of 11% at 880 nm and 18% at 370 nm (Supplement S4S3). The influence of the scattering material in the filter matrix, already included in the measurement uncertainty, could be reduced by explicitly taking into account the contribution of the scattering coefficient to the apparent absorption coefficient. However, this would require the knowledge of the particle size distribution, as the cross-sensitivity to scattering of the filter-based measurement depends on the particle size (Drinovec et al., 2015). The value of the multiple scattering parameter C (Weingartner et al., 2003; Drinovec et al., 2015; WMO, 2016) does not add to the final uncertainty because the same value is used for the calibration and the determination of mineral dust concentration, cancelling out in the final calculation.

600

605 However, the selection of the parameter C influences the calculation of mineral dust absorption coefficient and MAC . Similar to parameter C , the selected value of EF influences determination of absorption coefficients and MAC , but not the calculation of mineral dust concentration. It is the variation of EF , caused by the changes of the particle size distribution (Figure 5a), which induces about 18% uncertainty. This uncertainty can be reduced by using time-resolved measurements of EF or modifying the virtual impactor design to sharpen its response.

610 The main uncertainty comes from the variability of the chemical composition, mainly from the variability of ratio of Fe/Ca . This ratio is important because MAC of mineral dust depends mostly on the iron content, whereas calcium was used as a reference method for determination of mineral dust concentration. The SEM-EDX analysis of single particle chemical composition show large particle-to-particle variation inside the 24 h filter sample (Supplement S8). As expected the day-to-day variability of chemical composition is much lower as shown by ICP-MS analysis of trace metals (Supplement S7) - we obtained 40% variability of Fe/Ca ratio both for the campaign period as for the year-long dataset.

620 Desert dust may mix with BC emissions and this is relevant especially at source regions, where concentrations are large enough for efficient coagulation between dust and BC to occur (Clarke et al., 2004; Rodriguez et al., 2011), with up to a third of carbonaceous particles internally mixed with mineral dust (Hand et al., 2010). The presence of BC on large dust particles will increase the MAC of the coarse fraction. The presence of BC on dust means, that for these source regions, larger MAC values will be used to convert the optical measurements into dust concentrations. BC present on dust particles contributes negligibly to the mass and the resulting increase in PM_{10} concentrations is due to dust mass only. The increased MAC of these coagulated particles is also the relevant climate parameter, as dust and BC need to be taken into account together when estimating the direct radiative efficiency of such particles.

625 To reduce the uncertainty resulting from different MAC values, a mineral dust source location can be determined using back-trajectory analysis and an appropriate MAC should be used for each source location.

630 The combined uncertainty in determination of mineral dust concentration during the Cyprus campaign assuming independent contributions is 44%. The main reason for this uncertainty is the variation of the measured parameters used for the calibration of the method, essentially “—assuming the worst-case scenario”— of ever-changing aerosolized dust composition and resulting in an overestimation of the uncertainty. Alternatively, it is possible to derive the uncertainty from the measurement accuracy: to compare daily mineral dust concentrations obtained using VI-PM1 method with the reference values obtained using mass closure. This compares different methods measuring the same sample. Standard deviation of the ratio between predicted and reference mineral dust concentration was 29%. This is a quantification of the scatter of the regression ($R^2 = 0.92$) between the mineral dust concentrations determined using the two methods, as seen in Figure 87.

640 4. Conclusions

645 We have demonstrated the potential of the method by showing its applicability at a regional background site in Agia Marina Xyliiatou (Cyprus), frequently impacted by desert dust. We have shown how to determine the sample MAC and use it to quantify with high time resolution the contribution of desert dust to local PM_{10} concentrations.

650 Although black carbon contribution to the coarse mode is expected to be very small, internal mixture of dust and black carbon may potentially affect the MAC values determined by our methodology. On the other hand, it will not alter the capacity of our methodology to deliver high time resolution PM_{10} concentrations of dust. Instead, our measurement system will be calibrated with such aerosol mixture and a site-specific MAC value will be derived, that takes into account this mixing state. Our approach is particularly relevant when using dust optical properties in climate models which need to account for real-world MAC values to determine the heating of the atmosphere due to these aerosols.

660 The variability of our calibration methodology and therefore, the range of experimentally determined MAC values is currently investigated through long-term (multi-year) continuous observations at two regional background sites of the Mediterranean: Agia Marina Xyliatou (Cyprus) and Montseny (Spain). Such data will offer the unique opportunity to explore the factors controlling dust MAC values and in particular the influence of mineralogy of the different source regions (and especially their hematite and goethite content) and the potential impact of complex mixture of dust with black carbon.

665 Main conclusions are the following:

- An on-line method (named VI-PM1) for the determination of mineral dust concentration in ambient air based on absorption of coarse particles was developed.
- The VI-PM1 method was calibrated using mass closure performed on 24h filter samples yielding the uncertainty between 29% and 44%, using measurement accuracy and variation of the measured parameters, respectively.
- The VI-PM1 method allows for easy quantification of mineral dust in environments, where dust absorption is otherwise masked by absorption by black carbon in the fine aerosol fraction.
- During the campaign, we observed a continuous presence of mineral dust with an average of $8 \mu\text{g m}^{-3}$ and several intense events with concentrations up to $45 \mu\text{g m}^{-3}$.
- An average $MAC_{\text{mineral_dust},370\text{nm}}$ of $0.24 \pm 0.01 \text{ m}^2 \text{ g}^{-1}$ and Ångström exponent of 1.41 ± 0.29 were obtained for mineral dust measured at a background location in Cyprus. This seems to indicate that coarse fraction might be contaminated by black carbon.

680

Data availability. Campaign data can be accessed at the data repository of the Cyprus Institute using the following link: <https://mybox.cyi.ac.cy/public.php?service=files&t=624a471bf356165df49cad6cc747b051>.

685

Competing interests. Luka Drinovec and Griša Močnik were, at the time of the campaign, but not analysis and writing of the manuscript, also employed by the manufacturer of the Aethalometer AE33 Aerosol d.o.o. (Slovenia). The methodology was protected with the patent application.

690

Acknowledgements. This work was supported by Slovenian research agency (grant BI-FR/CEA/15-17-004 and programme P1-0099), and Slovenian Ministry of Economic Development and Technology, project DNAAP.

References

- Alfaro, S. C., Lafon, S., Rajot, J. L., Formenti, P., Gaudichet, A. and Maille', M.: Iron oxides and light absorption by pure desert dust: An experimental study. *J. Geophys. Res.*, 109, D08208, <https://doi:10.1029/2003JD004374>, 2004.
- Anderson, T. L. and Ogren, J. A.: Determining Aerosol Radiative Properties Using the TSI 3563 Integrating Nephelometer, *Aerosol Science and Technology*, 29:1, 57-69, doi: 10.1080/02786829808965551, 1998.
- Boucher, O., Randall, D., Artaxo, P., Bretherton, C., Feingold, G., Forster, P., Kerminen, V.-M., Kondo, Y., Liao, H., Lohmann, U., Rasch, P., Satheesh, S.K., Sherwood, S., Stevens, B. and Zhang, X.Y.: Clouds and Aerosols. In: *Climate Change 2013: The Physical Science Basis. Contribution of Working Group I to the Fifth Assessment Report of the Intergovernmental Panel on Climate Change* [Stocker, T.F., D. Qin, G.-K. Plattner, M. Tignor, S.K. Allen, J. Boschung, A. Nauels, Y. Xia, V. Bex and P.M. Midgley (eds.)]. Cambridge University Press, Cambridge, United Kingdom and New York, NY, USA. 2013.
- Bukowiecki, N., Hill, M., Gehrig, R., Zwicky, C. N., Lienemann, P., Hegedüs, F., Falkenberg, G., Weingartner, E., and Baltensperger, U.: Trace metals in ambient air: Hourly size-segregated mass concentrations determined by synchrotron-XRF, *Environ. Sci. Technol.*, 39, 5754–5762, <https://doi.org/10.1021/es048089m>, 2005.
- Caponi, L., Formenti, P., Massabó, D., Di Biagio, C., Cazaunau, M., Pangui, E., Chevaillier, S., Landrot, G., Andreae, M. O., Kandler, K., Piketh, S., Saeed, T., Seibert, D., Williams, E., Balkanski, Y., Prati, P., and Doussin, J.-F.: Spectral- and size-resolved mass absorption efficiency of mineral dust aerosols in the shortwave spectrum: a simulation chamber study, *Atmos. Chem. Phys.*, 17, 7175-7191, <https://doi.org/10.5194/acp-17-7175-2017>, 2017.
- Cavalli, F., Viana, M., Yttri, K. E., Genberg, J., and Putaud, J.-P.: Toward a standardised thermal-optical protocol for measuring atmospheric organic and elemental carbon: the EUSAAR protocol, *Atmos. Meas. Tech.*, 3, 79–89, <https://doi.org/10.5194/amt-3-79-2010>, 2010.
- Chen, B., Stein, A. F., Castell, N., Gonzalez-Castanedo, Y., Sanchez de la Campa, A. M., and de la Rosa, J. D.: Modeling and evaluation of urban pollution events of atmospheric heavy metals from a large Cu-smelter, *Sci. Total Environ.*, 539, 17–25, <https://doi.org/10.1016/j.scitotenv.2015.08.117>, 2016.
- [Clarke, A. D., Shinozuka, Y., Kapustin, V.N., Howell, S., Huebert, B., Doherty, S., Anderson, T., Covert, D., Anderson, J., Hua, X., Moore II, K. G., McNaughton, C., Carmichael, G., and Weber, R.: Size distributions and mixtures of dust and black carbon aerosol in Asian outflow: Physiochemistry and optical properties, *J. Geophys. Res.*, 109, D15S09, doi:10.1029/2003JD004378, 2004.](#)
- Collaud Coen, M., Weingartner, E., Schaub, D., Hueglin, C., Corrigan, C., Henning, S., Schwikowski, M., and Baltensperger, U.: Saharan dust events at the Jungfraujoch: detection by wavelength dependence of the single scattering albedo and first climatology analysis, *Atmos. Chem. Phys.*, 4, 2465-2480, <https://doi.org/10.5194/acp-4-2465-2004>, 2004.
- Cooper, J. A., Petterson, K., Geiger, A., Siemers, A., and Rupprecht, B.: Guide for developing a multi-metals, fenceline monitoring plan for fugitive emissions using X-ray based monitors, Cooper Environmental Services, Portland, Oregon, 1–42, , 2010.
- Derimian, Y., Karnieli, A., Kaufman, Y. J., Andreae, M. O., Andreae, T. W., Dubovik, O., Maenhaut, W., and Koren, I.: The role of iron and black carbon in aerosol light absorption, *Atmos. Chem. Phys.*, 8, 3623–3637, <https://doi.org/10.5194/acp-8-3623-2008>, 2008.
- Di Biagio, C., Formenti, P., Balkanski, Y., Caponi, L., Cazaunau, M., Pangui, E., Journet, E., Nowak, S., Andreae, M. O., Kandler, K., Saeed, T., Piketh, S., Seibert, D., Williams, E., and Doussin, J.-F.: Complex refractive indices and single-scattering albedo of global dust aerosols in the shortwave spectrum and relationship to size and iron content, *Atmos. Chem. Phys.*, 19, 15503–15531, <https://doi.org/10.5194/acp-19-15503-2019>, 2019.
- Di Biagio, C., Formenti, P., Cazaunau, M., Pangui, E., Marchand, N., and Doussin, J.-F.: Aethalometer multiple scattering correction Cref for mineral dust aerosols, *Atmos. Meas. Tech.*, 10, 2923–2939, <https://doi.org/10.5194/amt-10-2923-2017>, 2017.
- Di Mauro, B., Fava, F., Ferrero, L., Garzonio, R., Baccolo, G., Delmonte, B. and Colombo, R.: Mineral dust impact on snow radiative properties in the European Alps combining ground, UAV, and satellite observations, *J. Geophys. Res. Atmos.*, 120, 6080–6097, <https://doi.org/10.1002/2015JD023287>, 2015.
- Drinovec, L., Gregorič, A., Zotter, P., Wolf, R., Bruns, E. A., Prévôt, A. S. H., Petit, J.-E., Favez, O., Sciare, J., Arnold, I. J., Chakrabarty, R. K., Moosmüller, H., Filep, A., and Močnik, G.: The filter-loading effect by ambient aerosols in filter absorption photometers depends on the coating of the sampled particles, *Atmos. Meas. Tech.*, 10, 1043–1059, <https://doi.org/10.5194/amt-10-1043-2017>, 2017.

- Drinovec, L., Močnik, G., Zotter, P., Prévôt, A. S. H., Ruckstuhl, C., Coz, E., Rupakheti, M., Sciare, J., Müller, T., Wiedensohler, A., and Hansen, A. D. A.: The "dual-spot" Aethalometer: an improved measurement of aerosol black carbon with real-time loading compensation, *Atmos. Meas. Tech.*, 8, 1965-1979, <https://doi.org/10.5194/amt-8-1965-2015>, 2015.
- 750 Ealo, M., Alastuey, A., Ripoll, A., Pérez, N., Minguillón, M. C., Querol, X., and Pandolfi, M.: Detection of Saharan dust and biomass burning events using near-real-time intensive aerosol optical properties in the north-western Mediterranean, *Atmos. Chem. Phys.*, 16, 12567-12586, <https://doi.org/10.5194/acp-16-12567-2016>, 2016.
- 755 ECAC-report-IN-2015-1-5: https://www.actris-ecac.eu/files/ECAC-report-IN-2015-1-5_the-cyprus-institute_TSI3563-1082.pdf, last access: 17 June 2019, 2016.
- Engelbrecht, J. P., Moosmüller, H., Pincock, S., Jayanty, R. K. M., Lersch, T., and Casuccio, G.: Technical note: Mineralogical, chemical, morphological, and optical interrelationships of mineral dust re-suspensions, *Atmos. Chem. Phys.*, 16, 10809-10830, <https://doi.org/10.5194/acp-16-10809-2016>, 2016.
- 760 European Commission, Establishing guidelines for demonstration and subtraction of exceedances attributable to natural sources under the Directive 2008/50/EC on ambient air quality and cleaner air for Europe, SEC(2011) 208 final, Brussels, 15.02.2011, http://ec.europa.eu/environment/air/quality/legislation/pdf/sec_2011_0208.pdf, accessed 13 May 2019.
- 765 European Committee for Standardisation, EN 16909:2017 Ambient air - Measurement of elemental carbon (EC) and organic carbon (OC) collected on filters, CEN, Brussels, 2017.
- European Committee for Standardisation, EN 16913:2017 Ambient Air—Standard Method for the Measurement of NO₃⁻, SO₄²⁻, Cl⁻, NH₄⁺, Na⁺, K⁺, Mg²⁺, Ca²⁺ in PM_{2.5} as deposited on filters, CEN, Brussels, 2017.
- 770 Fang, G.C., Kuo, Y.C. and Zhuang, Y.J.: Source Analysis of Trace Metal Pollution Received at Harbor, Airport and Farmland Locations in Central Taiwan, *Aerosol Air Qual. Res.*, 15, 1774- 1786, <https://doi:10.4209/aaqr.2014.12.0314>, 2015.
- Fialho, P., Cerqueira, M., Pio, C., Cardoso, J., Nunes, T., Custódio, D., Alves, C., Almeida, S. M., Almeida-Silva, M., Reis, M., Rocha, F.: The application of a multi-wavelength Aethalometer to estimate iron dust and black carbon concentrations in the marine boundary layer of Cape Verde, *Atmos. Environ.*, 97, 136-143, <https://doi.org/10.1016/j.atmosenv.2014.08.008>, 2014.
- 775 Fialho, P., Freitas, M.C., Barata, F., Vieira, B., Hansen, A.D.A., Honrath, R.E.: The Aethalometer calibration and determination of iron concentration in dust aerosols, *J. Aerosol Sci.*, 37, 1497-1506. <http://dx.doi.org/10.1016/j.jaerosci.2006.03.002>, 2006.
- 780 Fialho, P., Hansen, A.D.A., Honrath, R.E.: Absorption coefficients by aerosols in remote areas: a new approach to decouple dust and black carbon absorption coefficients using seven-wavelength Aethalometer data, *J. Aerosol Sci.*, 36, 267-282, <http://dx.doi.org/10.1016/j.jaerosci.2004.09.004>, 2005.
- Formenti, P., Rajot, J. L., Desboeufs, K., Caquineau, S., Chevaillier, S., Nava, S., Gaudichet, A., Journet, E., Triquet, S., Alfaro, S., Chiari, M., Haywood, J., Coe, H. and Highwood, E.: Regional variability of the composition of mineral dust from western Africa: Results from the AMMA SOP0/DABEX and DODO field campaigns, *J. Geophys. Res.*, 113, D00C13, doi:10.1029/2008JD009903, 2008.
- 785 Greilinger, M., Schauer, G., Baumann-Stanzer, K., Skomorowski, P., Schöner, W. and Kasper-Giebl, A.: Contribution of Saharan Dust to Ion Deposition Loads of High Alpine Snow Packs in Austria (1987–2017). *Front. Earth Sci.* 6:126. <https://doi.org/10.3389/feart.2018.00126>, 2018.
- 790 Guieu, C., Lo'ye-Pilot, M.-D., Ridame, C., and Thomas, C.: Chemical Characterization of the Saharan dust end-member: Some biogeochemical implications for the Western Mediterranean sea, *J. Geophys. Res.*, 107, doi:10.1029/2001JD000582, 2002.
- Hand, V. L., Capes, G., Vaughan, D. J., Formenti, P., Haywood, J. M. and Coe, H.: Evidence of internal mixing of African dust and biomass burning particles by individual particle analysis using electron beam techniques, *J. Geophys. Res.*, 115, D13301, doi:10.1029/2009JD012938, 2010.
- 795 Herbert F., Dune, Chilton books, Philadelphia, 1965.
- Jeong, C.-H., Wang, J. M., and Evans, G. J.: Source Apportionment of Urban Particulate Matter using Hourly Resolved Trace Metals, Organics, and Inorganic Aerosol Components, *Atmos. Chem. Phys. Discuss.*, <https://doi.org/10.5194/acp-2016-189>, 2016.
- 800 Linke, C., Möhler, O., Veres, A., Mohácsi, Á., Bozóki, Z., Szabó, G., and Schnaiter, M.: Optical properties and mineralogical composition of different Saharan mineral dust samples: a laboratory study, *Atmos. Chem. Phys.*, 6, 3315–3323, <https://doi.org/10.5194/acp-6-3315-2006>, 2006.
- Mamali, D., Marinou, E., Sciare, J., Pikridas, M., Kokkalis, P., Kottas, M., Biniotoglou, I., Tsekeri, A., Keleshis, C., Engelmann, R., Baars, H., Ansmann, A., Amiridis, V., Russchenberg, H., and Biskos, G.: Vertical profiles of

- aerosol mass concentration derived by unmanned airborne in situ and remote sensing instruments during dust events, *Atmos. Meas. Tech.*, **11**, 2897–2910, <https://doi.org/10.5194/amt-11-2897-2018>, 2018.
- 805 Mamouri, R. E., Ansmann, A., Nisantzi, A., Kokkalis, P., Schwarz, A., and Hadjimitsis, D.: Low Arabian extinction-to-backscatter ratio, *Geophys. Res. Lett.*, **40**, 4762–4766, doi:10.1002/grl.50898, 2013.
- [Mani, M. and Pillai, R.: Impact of dust on solar photovoltaic \(PV\) performance: Research status, challenges and recommendations, *Renew. Sust. Energ. Rev.*, **14**, 3124–3131, <https://doi.org/10.1016/j.rser.2010.07.065>, 2010.](https://doi.org/10.1016/j.rser.2010.07.065)
- 810 Marinou, E., Tesche, M., Nenes, A., Ansmann, A., Schrod, J., Mamali, D., Tsekeri, A., Pikridas, M., Baars, H., Engemann, R., Voudouri, K.-A., Solomos, S., Sciare, J., Groß, S., Ewald, F., and Amiridis, V.: Retrieval of ice-nucleating particle concentrations from lidar observations and comparison with UAV in situ measurements, *Atmos. Chem. Phys.*, **19**, 11315–11342, <https://doi.org/10.5194/acp-19-11315-2019>, 2019.
- 815 Middleton, N., Yiallourous, P., Kleanthous, S., Kolokotroni, O., Schwartz, J., Dockery, D. W., Demokritou, P. and Koutrakis, P.: A 10-year time-series analysis of respiratory and cardiovascular morbidity in Nicosia, Cyprus: the effect of short-term changes in air pollution and dust storms, *Environ. Health*, **7**, 39, <https://doi.org/10.1186/1476-069X-7-39>, 2008.
- [Middleton, N. J.: Desert dust hazards: A global review, *Aeol. Res.*, **24**, 56–63, <https://doi.org/10.1016/j.aeolia.2016.12.001>, 2017.](https://doi.org/10.1016/j.aeolia.2016.12.001)
- 820 Myhre, G., Shindell, D., Bréon, F.-M., Collins, W., Fuglestvedt, J., Huang, J., Koch, D., Lamarque, J.-F., Lee, D., Mendoza, B., Nakajima, T., Robock, A., Stephens, G., Takemura, T. and Zhang, H.: Anthropogenic and Natural Radiative Forcing. In: *Climate Change 2013: The Physical Science Basis. Contribution of Working Group I to the Fifth Assessment Report of the Intergovernmental Panel on Climate Change* [Stocker, T.F., D. Qin, G.-K. Plattner, M. Tignor, S.K. Allen, J. Boschung, A. Nauels, Y. Xia, V. Bex and P.M. Midgley (eds.)]. Cambridge University Press, Cambridge, United Kingdom and New York, NY, USA, 2013.
- 825 Pandolfi, M., Cusack, M., Alastuey, A., and Querol, X.: Variability of aerosol optical properties in the Western Mediterranean Basin, *Atmos. Chem. Phys.*, **11**, 8189–8203, <https://doi.org/10.5194/acp-11-8189-2011>, 2011.
- 830 Pandolfi, M., Ripoll, A., Querol, X., and Alastuey, A.: Climatology of aerosol optical properties and black carbon mass absorption cross section at a remote high-altitude site in the western Mediterranean Basin, *Atmos. Chem. Phys.*, **14**, 6443–6460, <https://doi.org/10.5194/acp-14-6443-2014>, 2014.
- Park, S. S., Hansen, A. D. A., and Cho, Y.: Measurement of real time black carbon for investigating spot loading effects of Aethalometer data, *Atmos. Environ.*, **11**, 1449–1455, doi:10.1016/j.atmosenv.2010.01.025, 2010.
- 835 Perez, L., Tobías, A., Querol, X., Pey, J., Alastuey, A., Díaz, J., Sunyer, J.: Saharan dust, particulate matter and cause-specific mortality: A case–crossover study in Barcelona (Spain), *Environ. International* (48) 150–155, <https://doi.org/10.1016/j.envint.2012.07.001>, 2012.
- Phillips-Smith, C., Jeong, C.-H., Healy, R. M., Dabek-Zlotorzynska, E., Celo, V., Brook, J. R., and Evans, G.: Sources of particulate matter components in the Athabasca oil sands region: investigation through a comparison of trace element measurement methodologies, *Atmos. Chem. Phys.*, **17**, 9435–9449, <https://doi.org/10.5194/acp-17-9435-2017>, 2017.
- 840 Pikridas, M., Bezantakos, S., Močnik, G., Keleshis, C., Brechtel, F., Stavroulas, I., Demetriades, G., Antoniou, P., Vouterakos, P., Argyrides, M., Liakakou, E., Drinovec, L., Marinou, E., Amiridis, V., Vrekoussis, M., Mihalopoulos, N., and Sciare, J.: On-flight intercomparison of three miniature aerosol absorption sensors using unmanned aerial systems (UASs), *Atmos. Meas. Tech.*, **12**, 6425–6447, <https://doi.org/10.5194/amt-12-6425-2019>, 2019.
- 845 Pikridas, M., Vrekoussis, M., Sciare, J., Kleanthous, S., Vasiliadou, E., Kizas, C., Savvides, C., and Mihalopoulos, N.: Spatial and temporal (short and long-term) variability of submicron, fine and sub-10 μm particulate matter (PM₁, PM_{2.5}, PM₁₀) in Cyprus, *Atmos. Environ.*, **191**, 79–93, <https://doi.org/10.1016/j.atmosenv.2018.07.048>, 2018.
- 850 Poulakis, E., Theodosi, C., Bressi, M., Sciare, J., Ghersi, V., and Mihalopoulos, N.: Airborne mineral components and trace metals in Paris region: spatial and temporal variability. *Environ Sci Pollut R*, **22**(19), 14663–14672, 2015.
- Rodríguez, S., Querol, X., Alastuey, A., Kallos, G., Kakaliagou, O.: Saharan dust contributions to PM₁₀ and TSP levels in Southern and Eastern Spain, *Atmos. Environ.* (35), 2433–2447, [https://doi.org/10.1016/S1352-2310\(00\)00496-9](https://doi.org/10.1016/S1352-2310(00)00496-9), 2001.
- 855 [Rodríguez, S., Alastuey, A., Alonso-Pérez, S., Querol, X., Cuevas, E., Abreu-Afonso, J., Viana, M., Pérez, N., Pandolfi, M., and de la Rosa, J.: Transport of desert dust mixed with North African industrial pollutants in the subtropical Saharan Air Layer, *Atmos. Chem. Phys.*, **11**, 6663–6685, <https://doi.org/10.5194/acp-11-6663-2011>, 2011.](https://doi.org/10.5194/acp-11-6663-2011)
- 860

[Scarnato, B. V., China, S., Nielsen, K., and Mazzoleni, C.: Perturbations of the optical properties of mineral dust particles by mixing with black carbon: a numerical simulation study, *Atmos. Chem. Phys.*, 15, 6913–6928, <https://doi.org/10.5194/acp-15-6913-2015>, 2015.](#)

- 865 Schauer, G., Kasper-Giebl, A., and Močnik, G. Increased PM concentrations during a combined wildfire and Saharan dust event observed at high-altitude sonnblick observatory, Austria. *Aerosol Air Qual. Res.* 16, 542–554. doi: 10.4209/aaqr.2015.05.0337, 2016.
- Schrod, J., Weber, D., Drücke, J., Keleshis, C., Pikridas, M., Ebert, M., Cvetković, B., Nickovic, S., Marinou, E., Baars, H., Ansmann, A., Vrekoussis, M., Mihalopoulos, N., Sciare, J., Curtius, J., and Bingemer, H. G.: Ice nucleating particles over the Eastern Mediterranean measured by unmanned aircraft systems, *Atmos. Chem. Phys.*, 17, 4817–4835, <https://doi.org/10.5194/acp-17-4817-2017>, 2017.
- 870 Sciare, J., D'Argouges, O., Esteve, R. S., Gaimoz, C., Dolgorouky, C., Bonnaire, N., Favez, O., Bonsang, B., and Gros, V.: Large contribution of water insoluble secondary organic aerosols in the region of Paris (France) during wintertime, *J. Geophys. Res.*, 116, D22203, doi:10.1029/2011JD015756, 2011.
- 875 Sciare, J., Oikonomou, K., Cachier, H., Mihalopoulos, N., Andreae, M. O., Maenhaut, W., and Sarda-Estève, R.: Aerosol mass closure and reconstruction of the light scattering coefficient over the Eastern Mediterranean Sea during the MINOS campaign, *Atmos. Chem. Phys.*, 5, 2253–2265, <https://doi.org/10.5194/acp-5-2253-2005>, 2005.
- Sioutas, C., Koutrakis, P., Burton, R.M.: Development of a low cutpoint slit virtual impactor for sampling ambient fine particles, *Journal Aerosol Sci.*, 25, 1321-1330, [https://doi.org/10.1016/0021-8502\(94\)90128-7](https://doi.org/10.1016/0021-8502(94)90128-7). 1994.
- 880 Sokolik, I. and Toon, O.: Incorporation of mineralogical composition into models of the radiative properties of mineral aerosol from UV to IR wavelengths, *J. Geophys. Res.*, 104, 9423–9444, 1999.
- Valenzuela, A., Olmo, F. J., Lyamani, H., Antón, M., Titos, G., Cazorla, A., and Alados-Arboledas, L.: Aerosol scattering and absorption Angström exponents as indicators of dust and dust-free days over Granada (Spain), *Atmos. Res.*, 154, 1– 13, <https://doi.org/10.1016/j.atmosres.2014.10.015>, 2015.
- 885 Viana, M., Salvador, P., Artíñano, B., Querol, X., Alastuey, A., Pey, J., Latz, A. J., Cabañas, M., Moreno, T., Dos Santos, S. G., Herce, M. D., Hernández, P. D., García D. R., and Fernández-Patier, R.: Assessing the Performance of Methods to Detect and Quantify African Dust in Airborne Particulates, *Environ. Sci. Tech.* 44 , 8814-8820, <https://doi.org/10.1021/es1022625>, 2010.
- 890 Visser, S., Slowik, J. G., Furger, M., Zotter, P., Bukowiecki, N., Canonaco, F., Flechsig, U., Appel, K., Green, D. C., Tremper, A. H., Young, D. E., Williams, P. I., Allan, J. D., Coe, H., Williams, L. R., Mohr, C., Xu, L., Ng, N. L., Nemitz, E., Barlow, J. F., Haliou, C. H., Fleming, Z. L., Baltensperger, U., and Prévôt, A. S. H.: Advanced source apportionment of size-resolved trace elements at multiple sites in London during winter, *Atmos. Chem. Phys.*, 15, 11291–11309, <https://doi.org/10.5194/acp-15-11291-2015>, 2015a.
- 895 Vrekoussis, M., Liakakou, E., Koçak, M., Kubilay, N., Oikonomou, K., Sciare, J., Mihalopoulos, N.: Seasonal variability of optical properties of aerosols in the Eastern Mediterranean, *Atmo. Environ.* 39, 7083-7094, <https://doi.org/10.1016/j.atmosenv.2005.08.011>, 2005.
- Weingartner, E., Saathoff, H., Schnaiter, M., Streit, N., Bitnar, B., and Baltensperger, U.: Absorption of light by soot particles: determination of the absorption coefficient by means of aethalometers, *J. Aerosol Sci.*, 34, 1445–1463, doi:10.1016/S0021-8502(03)00359-8, 2003.
- 900 WHO, Workshop: Evaluating the short-term health effects of desert and anthropogenic dust, 29 October 2018, Geneva, WHO.
- WMO, Report No. 227: WMO/GAW Aerosol Measurement Procedures, Guidelines and Recommendations, 2nd Edition, 2016, Geneva, WMO.
- 905 Zhang, X. Y., Wang, Y. Q., Zhang, X. C., Guo, W., Niu, T., Gong, S. L., Yin, Y., Zhao, P., Jin, J. L., and Yu M.: Aerosol monitoring at multiple locations in China: contributions of EC and dust to aerosol light absorption, *Tellus B: Chemical and Physical Meteorology*, 60:4, 647-656, doi:10.1111/j.1600-0889.2008.00359.x, 2008.

Supplement for the manuscript: A new optical-based technique for real-time measurements of mineral dust concentration in PM10 using a virtual impactor

S1. Virtual Impactor Characterization

5

The performance of the virtual impactor (VI) was characterized using NIST polystyrene-latex (PSL) spheres with nominal aerodynamic sizes from 0.7 to 10 μm . A schematic of the experimental setup is provided in Figure S1. In brief, particles produced by atomization were consequently dried and their number distribution was measured using an Aerodynamic Particle Counter (APS; TSI mod 3321). The APS was operated with 5 (nominal) and with 1.5 (modified) l min^{-1} sampling flows. The VI was respectively operated at 95 (maximum available) and 75 l min^{-1} , providing total-to-minor flow ratios of 19 (i.e., 95:5) and 50 (i.e., 75:1.5). Since the atomizer used was not capable of providing the above-mentioned total flows, a "Y" junction with a HEPA filter was used downstream the silica diffusion drier for supplementing air into the system (i.e., dilution). For maintaining the total flow and thus the dilution and the particle losses in the system constant, the high flow of the VI was always operational. The concentration of particles was measured before and after the VI using another "Y" junction. For measurements of the particle concentration with the VI, the APS was connected in the minor flow outlet of the VI, while a closed valve was used to block the other outlet of the second "Y" junction (Figure S1 a). Particle concentration before the impactor was measured by connecting the APS directly to the Y junction (i.e., upstream the VI), while the closed valve was put to the low flow outlet of the VI (Figure S1 b). Note that, in the latter case the high flow of the VI was operational as well for maintaining the total flow of the system constant.

10

15

20

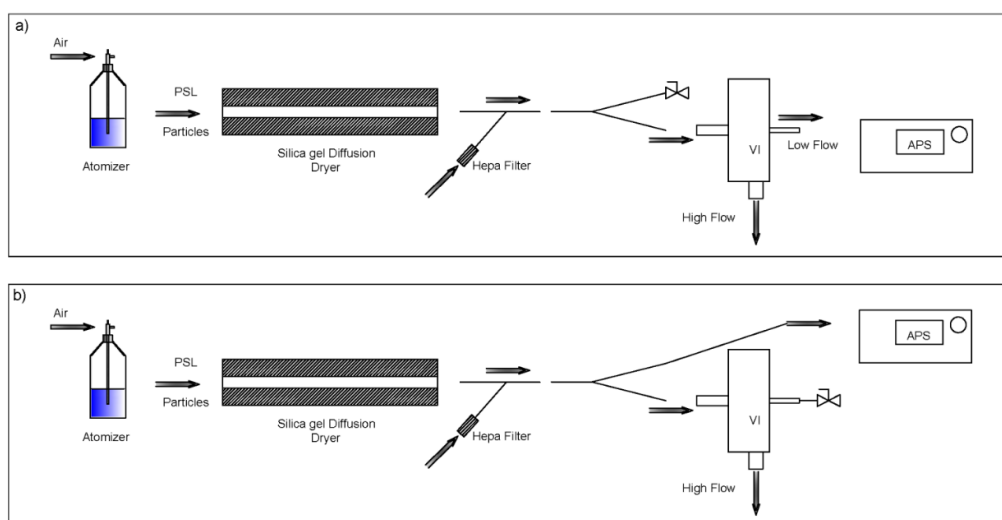


Figure S1. Schematics of the experimental setup for characterizing the performance of the virtual impactor. Particle size distributions were measured using an APS downstream (a) and upstream the VI (b). In both cases the high flow of the VI was operational for maintaining the total flow and consequently the dilution and particle losses in the system constant.

25

Five samples were collected in each case (i.e., size distribution measured downstream and upstream the VI) for each PSL size and for each set of flow rates. The average measured size distributions were used for calculating the concentration enhancement factor CE of the VI at the specific aerodynamic diameters (D), corresponding to the aerodynamic diameters of PSL particles used in each experiment as follows:

30

$$CE(D) = \frac{c_{VI}}{c} \quad . \quad (S1)$$

The fraction of theoretical concentration efficiency fCE , defined as the ratio of the concentration efficiency calculated for each aerodynamic diameter D , with the virtual impactor flow ratio FR (maximum efficiency) was also calculated as follows:

35

$$FR = \frac{F_{in}}{F_{out}} \quad , \quad (S2)$$

$$fCE(D) = \frac{CE(D)}{FR} \quad . \quad (S3)$$

40

Figure 2 shows the results in terms of the enhancement factor for particles having nominal diameter from 0.7 to 10 μm when the VI was operated at two different flow settings, namely 95:5 and 75:1.5 l min^{-1} (i.e., total:minor flow), respectively. Note that, the enhancement factor of 0.5 μm was calculated from the size distributions obtained from measuring particles with nominal diameter of 0.7 μm and that for the flow settings of 75:1.5 l min^{-1} the maximum size of particles measured was 5 μm .

45

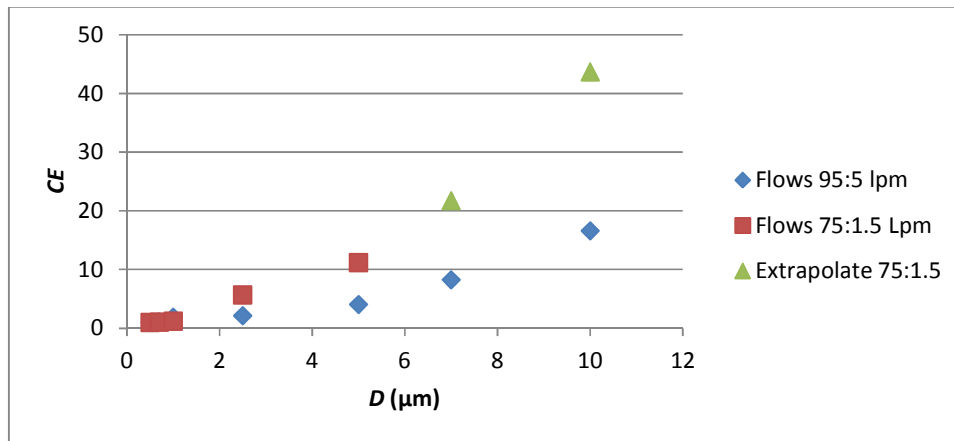
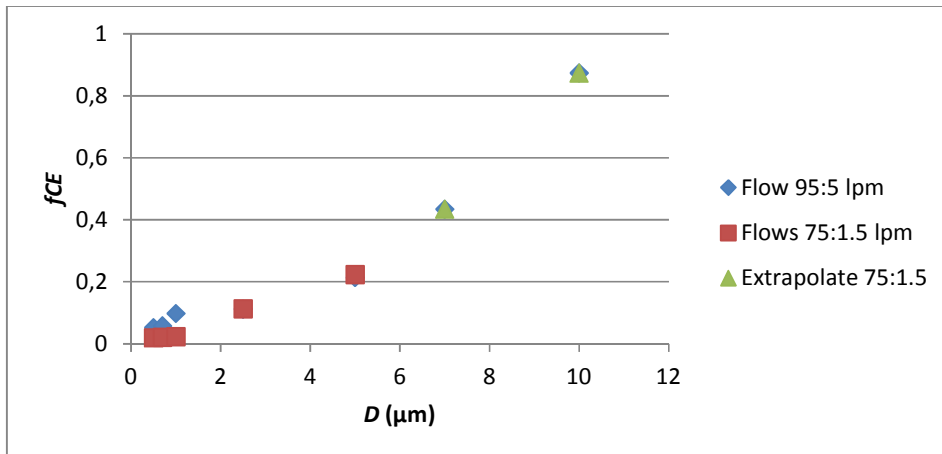


Figure S2. Concentration efficiency for particles having aerodynamic diameters ranging from 0.7 to 10 μm when the VI was operated with 95:5 and 75:1.5 l/min , total:minor flow, respectively. For the larger flow, the enhancement factor:concentration efficiency of the larger particles (i.e., 7, 10 μm) is not measured but extrapolated due to poor counting statistics.

50

55 Figure S3 shows the results in terms of the fraction of theoretical concentration efficiency (f_{CE}) for the measured particles when the VI was operated at two different flow settings. While the measured concentration efficiency is different at each measured size and for each set of flows, the calculated f_{CE} is almost identical for each size. This suggests that the enhancement factor of the VI for particle sizes above 1 μm can be estimated if the flow ratio is known. Table S1 shows aggregate results of the experiments conducted and used for producing Figures S1 and S2.

60



65 Figure S3. Fraction of the theoretical concentration efficiency (f_{CE}) for particles having aerodynamic diameters ranging from 0.7 to 10 μm when the VI was operated with flow ratios 95:5 and 75:1.5, respectively. For the larger flow, the concentration efficiency of the larger particles (i.e., 7, 10 μm) is not measured but extrapolated due to poor counting statistics.

70 Table S1. Aggregate results of the concentration efficiency (CE) and fraction of the theoretical concentration efficiency (f_{CE}) of particles having aerodynamic diameters ranging from 0.7 to 10 μm , when the VI was operated with 95:5 and with 75:1.5 flow ratios. Green values are extrapolated.

D (μm)	Experiment 1 ($F_{in}=75 \text{ l min}^{-1}$, $F_{out}=1.5 \text{ l min}^{-1}$, $FR=50$)		Experiment 2 ($F_{in}=95 \text{ l min}^{-1}$, $F_{out}=5 \text{ l min}^{-1}$, $FR=19$)	
	CE	f_{CE}	CE	f_{CE}
0.5	1.00	0.0200	1.00	0.0526
0.7	1.06	0.0212	1.11	0.0584
1	1.20	0.0240	1.87	0.0984
2.5	5.68	0.1135	2.14	0.1126
5	11.19	0.2238	4.07	0.2142
7	21.74	0.4347	8.26	0.4347
10	43.68	0.8737	16.60	0.8737

75

S2. Filter loading effect compensation on AE33 with virtual impactor

80

The automatic compensation of the AE33 failed for the VI measurements and produced faulty values of the compensation parameter k due to the quantum nature of big particles: particles are directed either to spot 1 or spot 2 in the optical chamber of the instrument. Because of the size of these particles, they induce a large signal on one measurement spots at the time (Figure S4), which hinders automatic compensation algorithm (Drinovec et al., 2015) – see variation of parameter k values during the campaign (Figure S5a).

85

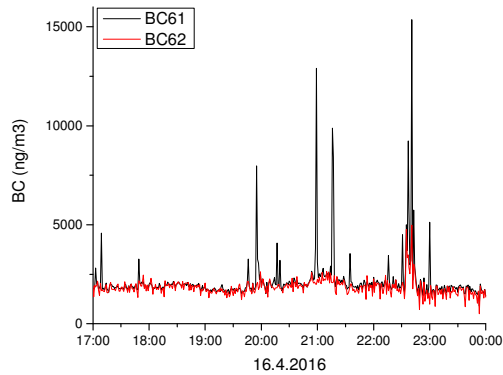
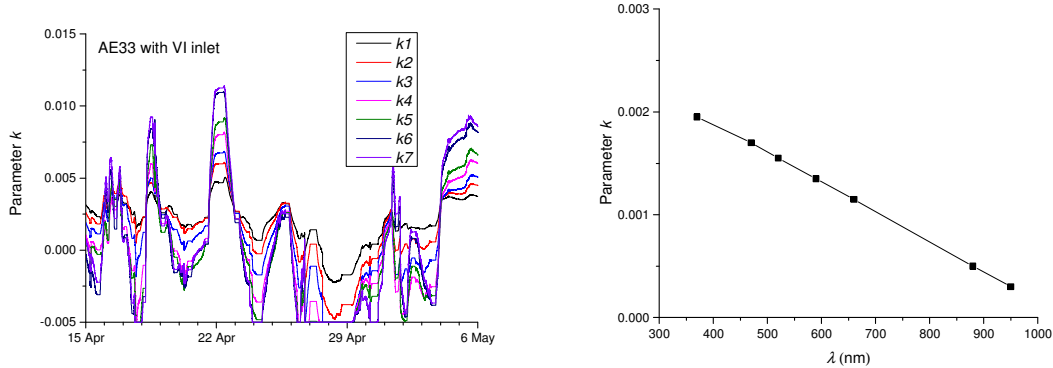


Figure S4. Signal from AE33 connected to the virtual impactor for spot 1 and spot 2.

The loading effect was characterized using the BC vs. ATN method (Park et al., 2010; Drinovec et al., 2015) using the data between 16 April 2016 and 30 April 2016. The obtained slopes (Figure S2) are used for offline compensation using equation $cBC=BC/(1-k*ATN)$. The compensated data is again tested using the BC vs. ATN method (Figure S6).

90

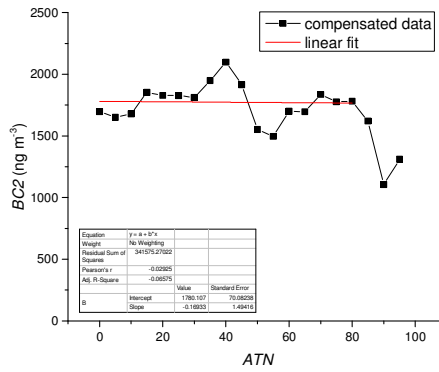
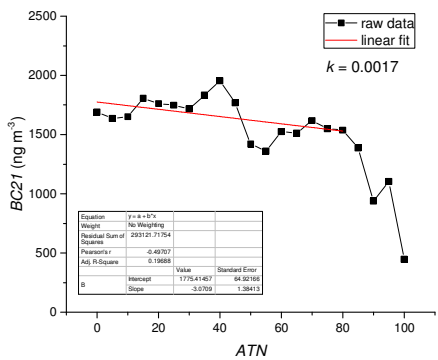


a)

b)

95

Figure S5. The compensation parameter k values determined by AE33 (a) and those used for offline compensation of data from Aethalometer with a virtual impactor inlet (b).



100

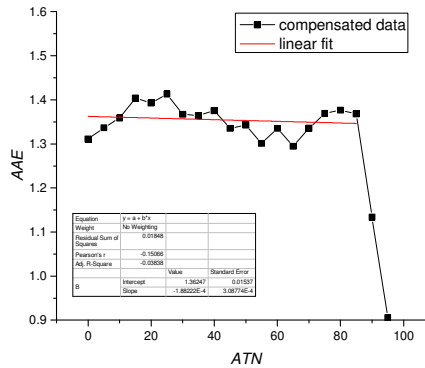
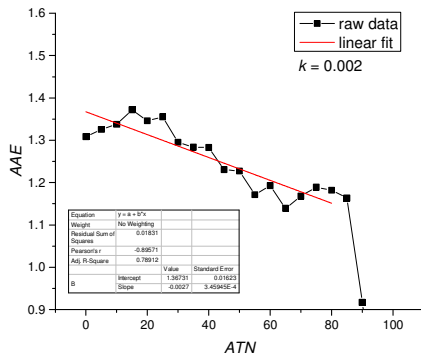
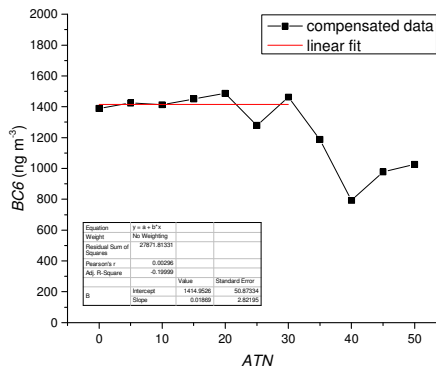
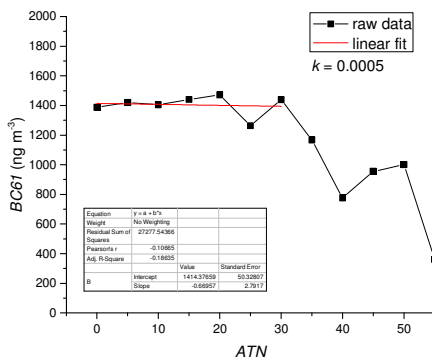
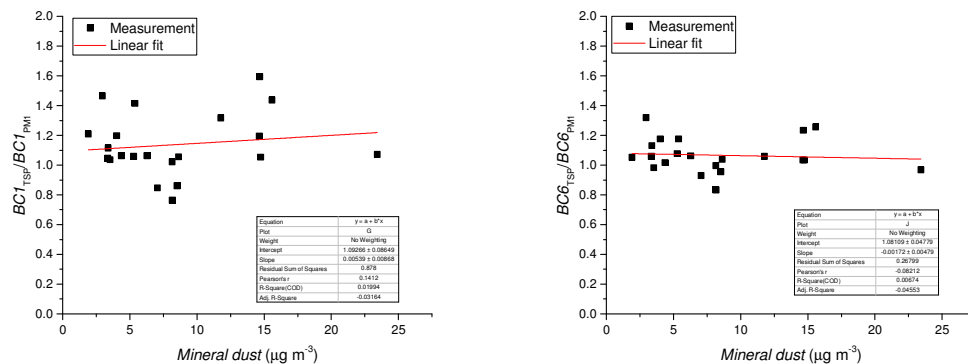


Figure S6. BC vs. ATN analysis for raw data (left side) and data compensated using fixed k values, derived from the left plot (right side).

105

S3. Uncertainty of AE33 measurements

The uncertainty of AE33 measurements was determined calculating the ratio of BC between instrument with TSP and PM_{10} inlets. Because there is almost no dependence of $BC_{TSP}/BC_{PM_{10}}$ ratio on mineral dust concentration (Figure S7), the variation of this parameter results from the measurement uncertainty. Uncertainty of BC during the Cyprus campaign is thus calculated as a standard deviation of $BC_{TSP}/BC_{PM_{10}}$ ratio (Table S2).



a)

b)

Figure S7. Correlation between 24h average ratios $BC_{TSP}/BC_{PM_{10}}$ and Mineral dust concentration for Aethalometer channel 1 (a) and channel 6 (b).

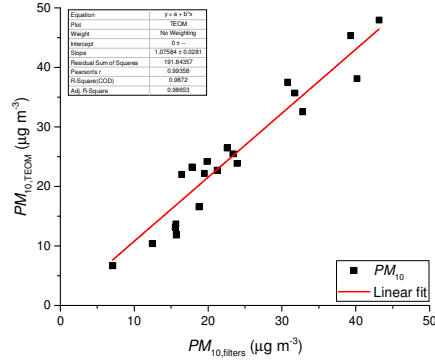
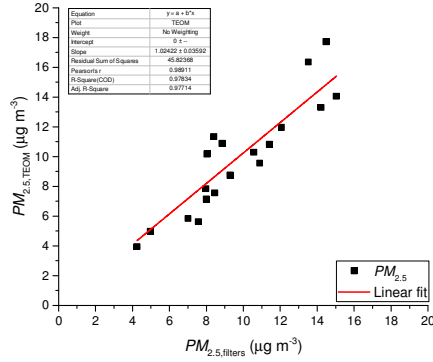
Table S2. Uncertainty estimation during the Cyprus campaign

Wavelength	$BC_{TSP}/BC_{PM_{10}}$	Uncertainty for BC
370 nm	1.14 ± 0.21	18%
880 nm	1.07 ± 0.12	11%

S4. Correlation between *PM* measurements by TEOM and filter weighting

120

TEOM and filter measurements data obtained between 15 April 2016 and 6 May 2016 are compared (Figure S8, Table S3). The two methods show high R^2 value and a slope which differs from unity by less than 10%. On average TEOM overestimates *PM* by 2% for $PM_{2.5}$ and 8% for PM_{10} .



125

a)

b)

Figure S8. Correlation between $PM_{2.5}$ (a) and PM_{10} (b) measured by TEOM and filter weighting.

Table S3. Fitting results for correlation between TEOM and filter weighting method.

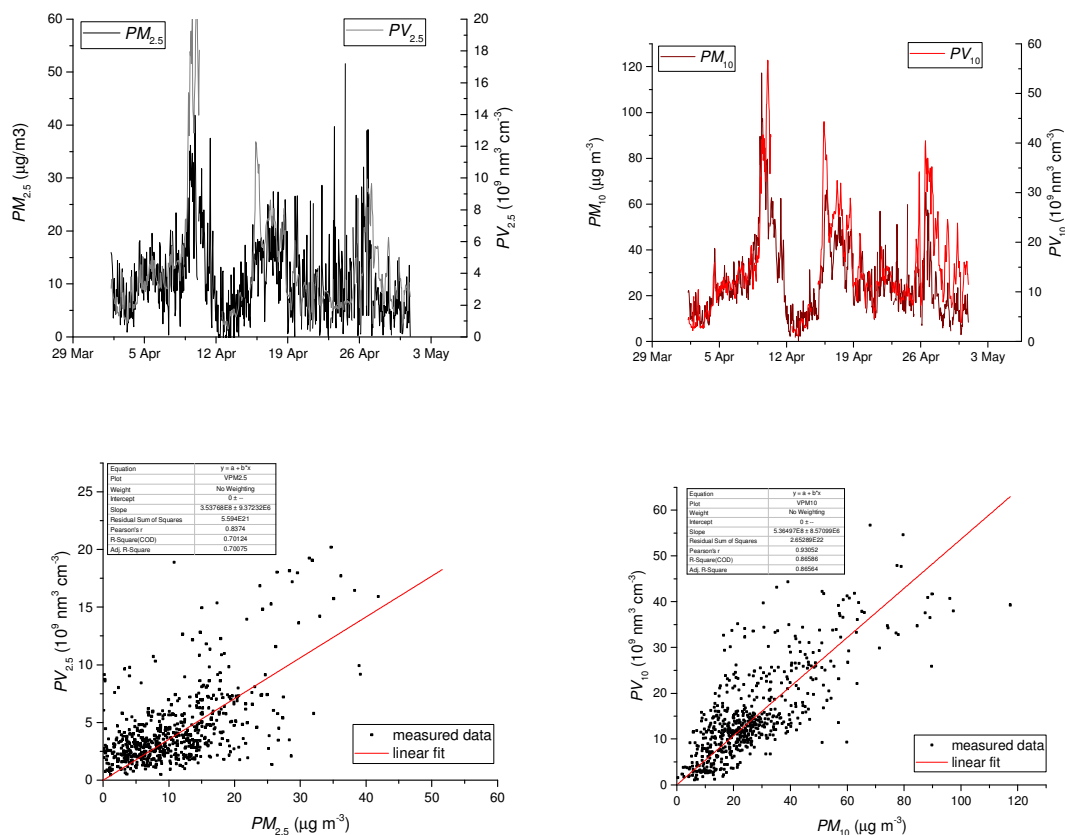
130

	<i>Slope</i>	R^2
$PM_{2.5}$	1.02 ± 0.04	0.978
PM_{10}	1.08 ± 0.03	0.987

135 **55. Correlation between APS and TEOM**

The aerodynamic particle size distribution from APS was used to calculate particle volume for PM_{10} and $PM_{2.5}$ size fraction assuming the sphericity of the particles. Particle volume was compared with the particle mass concentrations $PM_{2.5}$ and PM_{10} obtained by TEOM (Figure S9). The correlation is better for sub 10 μm size fraction with R^2 of 0.97. The sub 2.5 μm fraction has a 33% smaller volume/mass slope compared to the sub 10 μm fraction.

140



145

Figure S9. Time series of particle mass concentration (PM) and particle volume concentration (PV) concentrations in 2.5 μm and 10 μm size fractions (a,b) and correlations (c,d).

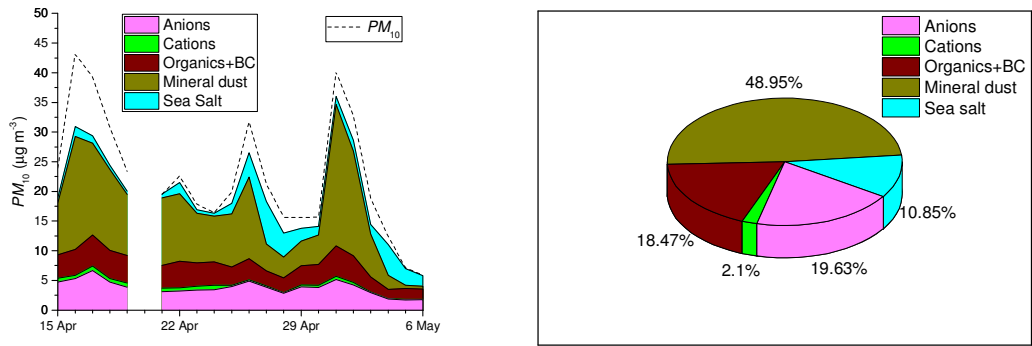
150

Table S4 . Fitting results for correlation between APS and TEOM.

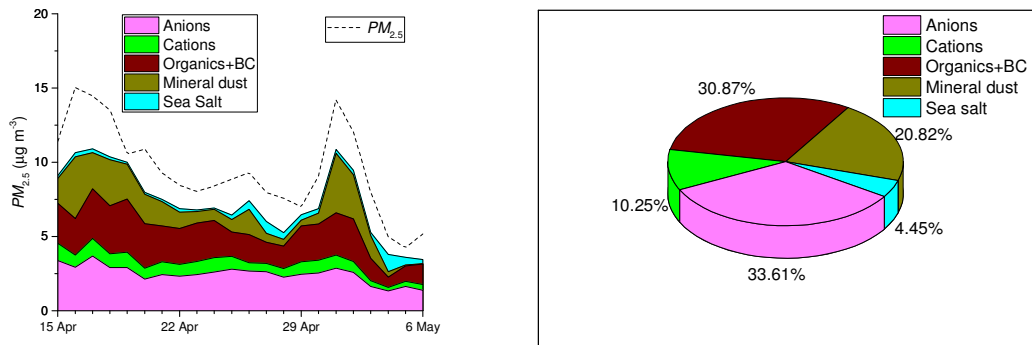
Correlation	Slope ($\mu m^{-3} \mu g^{-1}$)	R^2
PV_{10} vs. PM_{10}	$5.36E5 \pm 9E3$	0.87
$PV_{2.5}$ vs. $PM_{2.5}$	$3.54E5 \pm 9E3$	0.70

S6. Mass closure on daily PM10 samples

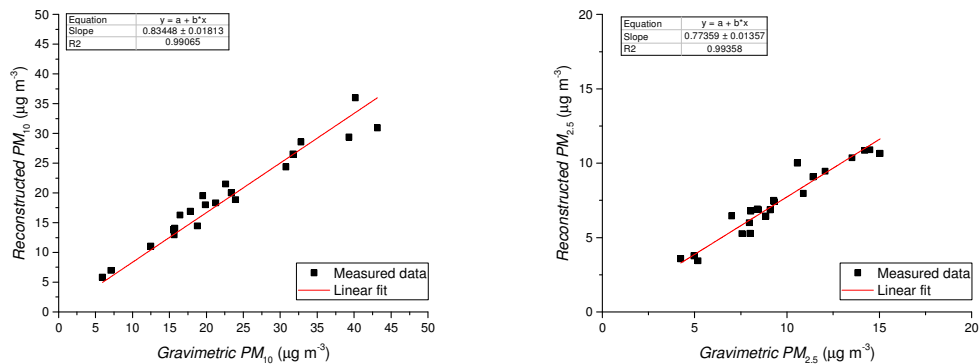
155 Mass closure was performed by combining PM_{10} from the high volume sampler filters, chemical analysis for cations (NH_4^+ , K^+) and anions (NO_3^- , SO_4^{2-}). Calcium concentration was used to establish mineral dust concentration assuming its 12% mass fraction in mineral dust. Organic matter was calculated from organic carbon concentration (OC) using a organic mass-to-organic carbon factor of 2.



160 a) b) **Figure S10. Time series (a) and average (b) contributions of different components to PM_{10} (a) during the measurement campaign.**



165 a) b) **Figure S11. Time series (a) and average (b) contributions of different components to $PM_{2.5}$ (a) during the measurement campaign.**



a) b) **Figure S12. Correlation between gravimetric measurements of PM and that reconstructed from chemical analysis.**

170 **S7. Trace element analysis on PM₁₀ filters using inductively coupled plasma mass spectrometry (ICP-MS)**

24h PM₁₀ filters were analysed for trace elements As, Cd, Pb, Ni, Cr, Fe, Cu, Al, V, Mn, Zn and Ti. Al and Fe can be used to identify mineral dust (Guieu et al., 2002), showing good correlation with Ca obtained by ion chromatography (Figure S13). for the whole year 2016 we obtained average slope between Al and Ca of 0.58 ± 0.01 and average slope between Fe and Ca of 0.44 ± 0.01 (Figure S14).

175

Statistical analysis of chemical ratio Fe/Ca can give us information on the variability of chemical composition of mineral dust (Table S5) and directly influences the accuracy of the VI-PM1 method.

180

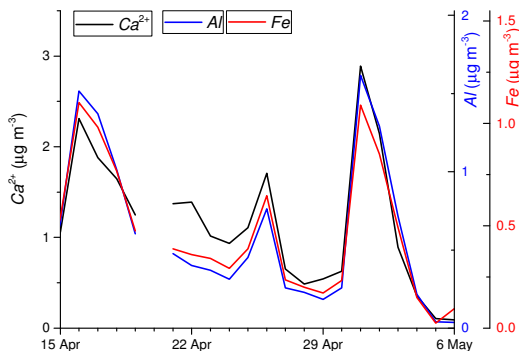
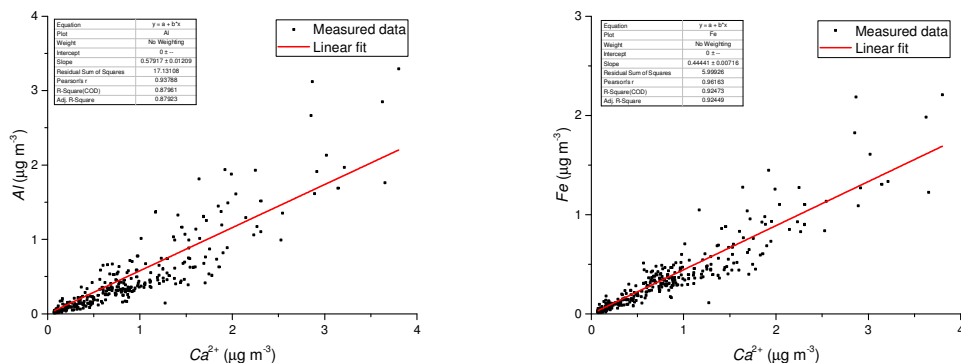


Figure S13. Time series of ambient Ca²⁺, Al and Fe concentration in PM₁₀ fraction during the calibration campaign



185 **Figure S14. Correlation between Al (a) and Fe (b) with Ca measured on 24h PM₁₀ filters. The figures contain data for the whole year 2016.**

Table S5. Elemental composition and ratios for iron, calcium and aluminium for the whole 2016 and for the calibration part of the Cyprus campaign.

190

	Year 2016	Variability	Interval 16.4.2016 – 6.5.2016	Variability
Fe/PM ₁₀	0.015 ± 0.008	53%	0.019 ± 0.006	32%
Ca/PM ₁₀	0.037 ± 0.017	46%	0.047 ± 0.016	34%
Fe/Ca	0.41 ± 0.15	38%	0.42 ± 0.17	40%

S8. Characterization of mineral dust using scanning electron microscopy – energy dispersive X-ray (SEM-EDX) analysis of PM_{10} filters

195

Several filter samples were analyzed for their elemental composition using energy-dispersive X-ray spectroscopy – similarly to Engelbrecht et al. (2016). An example of SEM-EDX measurement is presented on Figure S15. Each of the selected filter samples was characterized by an average of 10-20 SEM-EDX analyses (Figure S16). The main constituent elements of mineral dust in all filters are oxygen, silica and aluminium. There is a big particle-to-particle variation in the elemental composition. With a higher number of collected particles the uncertainty of the elemental composition is reduced.

200

The sample from 10 April 2016 contains sodium and chlorine indicating the influence of sea salt. Calcium (0-10%), iron (0-5%) and potassium (0.5-2%) contributions differ a lot between the different filters. Formenti et al. (2008) showed a similar variability of mineral composition for dust from different source regions.

205

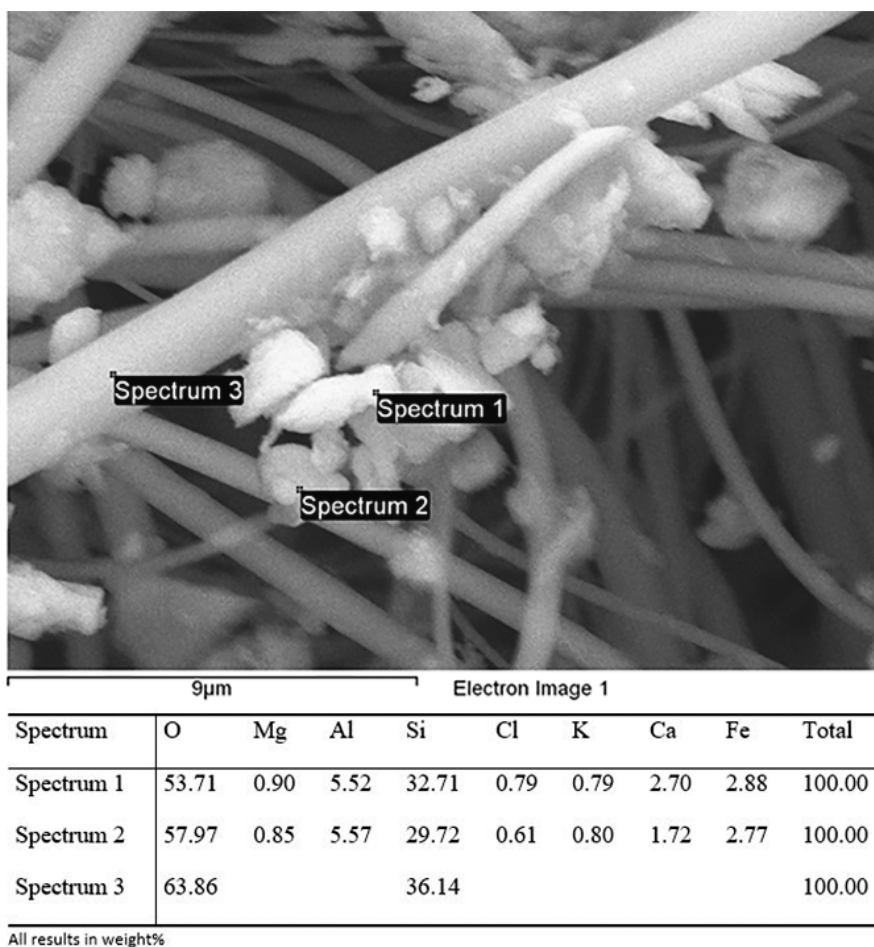
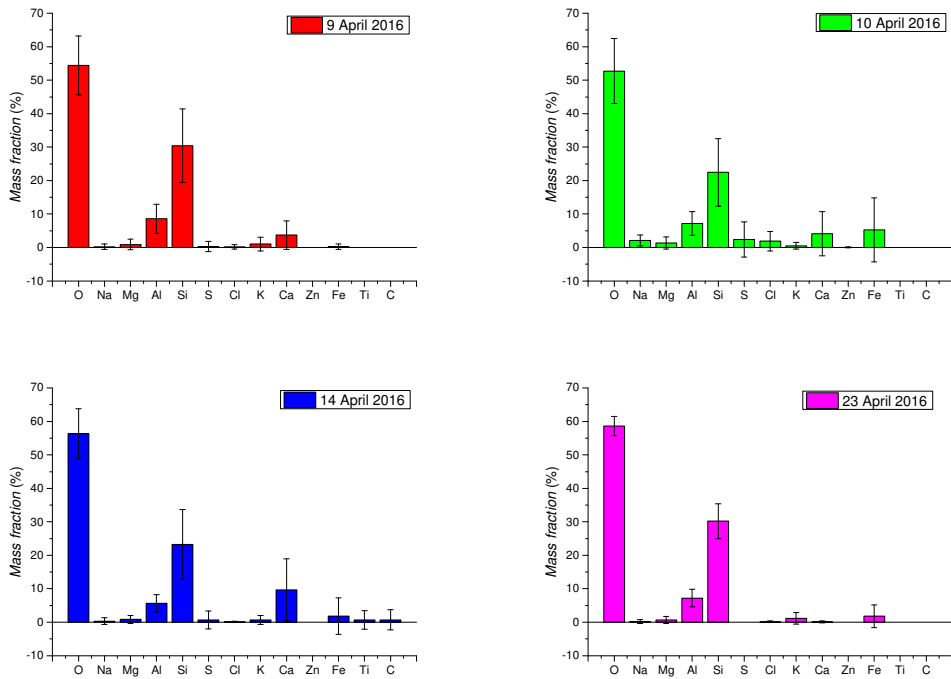


Figure S15. SEM-EDX analysis of particles (Spectrum 1 & 2) collected on the quartz fiber filter (Spectrum 3).

210



215

Figure S16. Elemental composition of mineral dust filter samples obtained using EDX spectroscopy. The error bars show the standard deviation of 10-20 measurements on each sample.